NTNU
Norwegian University of Science and Technology
Department of Marine Technology

# M.Sc.THESIS

| Title: | Delivered: |
|---|---|
| **Lowering operation of a subsea module using air filled suction anchors to reduce the crane load capacity required.** | 14.06.2010 |
| | **Availability:** Open |
| **Student:** Henrik Kvadsheim | **Number of pages:** 83 |

**Abstract:**

The Ormen Lange gas field is located 120 km west-north west of Kristiansund, and went in to production in October 2007. The field is planned to be developed throughout 2015 including the installation of a subsea compression station, SCS to boost well stream to maintain production. The challenges of installing the SCS are the depth of 890 meters at the Ormen Lange field and the weight of 8000 tonne of the SCS.

Aker Marine Contractors, AMC has developed a unique method for lowering the SCS through the sea surface and further down. The method involves the use of trapped air inside the suction anchors, SAs in order to reduce the crane load capacity required. The compressibility of the trapped air however, means that this buoyancy force will not be constant but reduce as the SCS is lowered down. The change in buoyancy force is largest close to the sea surface.

A simple model of the lowering operation of the SCS has been developed and it formed the basis for the design basis. The design basis was used to simulate the lowering operation in the time domain program SIMO. Two simulations of the same lowering operation were performed, one in still water and one in worst weather conditions. The SIMO models successfully included the change in behavior of the trapped air as the SAs went from floating to submerged. The simulations showed that the reduction of buoyancy force due to the trapped air as the SCS was lowered through the surface was smaller than the cranes could safely handle.

A model test setup of the same lowering operation has been suggested. The test was divided into two parts: Part 1 where a model setup of the lowering operation of the SCS through the sea surface were suggested but concluded to not be a good solution. Part 2 where a model setup of the SCS which by performing a decay test could find the hydrodynamics loads such as added mass and damping. This model test was concluded not to be necessary in term of improving the SIMO model due the lowering operation may be viewed as a static problem. To actually perform a model test was not a part of this thesis.

**Keyword:**

SIMO
Compressibility of air

**Advisor:**

Professor II Tor Einar Berg

Address:
NTNU
Department of Marine Technology

Location
Marinteknisk Senter
O. Nielsens vei 10

Tel. +47 73 595501
Fax +47 73 595697

## MSc thesis, spring 2010

for

Henrik Kvadsheim

## Lowering operation of a subsea module using air filled suction anchors to reduce the crane load capacity required.

AMC has developed a unique method for lowering a subsea module called SCS through the sea surface and further down. The method involves the use of trapped air inside the SAs in order to reduce the crane load capacity required. The compressibility of the trapped air however, means that this buoyancy force will not be constant but reduce as the SCS is lowered down. The change in buoyancy force is largest close to the sea surface.

The main focus of this thesis will be to reduce the complex lowering operation of the SCS to a simplified model for use as a design basis. This simplified model will be used to simulate the lowering operation in the time domain program SIMO. A model test setup of the same operation will be suggested. To actually perform a model test is not a part of this thesis.

### Scope of work

1. Define the case to be modeled – the lowering operation of the SCS through the sea surface.
2. Develop mathematical models for predicting how the trapped air will behave.
3. Describe a model test setup of the lowering operation.
4. Describe the SCS and the barges used in the lowering operation.
5. Develop a simplified model of the complex lowering operation for use as a design basis for a time domain simulation.
6. Generate a time domain simulation of the lowering operation using SIMO.
7. Discuss the result from the SIMO simulation and how a model test would compliment, improve or verify these results.

The report shall be written in English and include a description of mathematical models and of a model test set up, description of the design basis, discussion of the SIMO simulation results and a conclusion including a proposal for further work. Source code will be provided on a CD code listing enclosed in appendix.

The thesis should be well organized and give a clear presentation of the work and all conclusions. It is important that the text is well written and that tables and figures are used to support the verbal presentation. The thesis should be complete, but still as short as possible.

The thesis will be submitted in two paper copies signed by the candidate and a third digital copy within 14. June 2010.

Advisor: Peter Christian Sandvik, Stefan Schlomilch and Helge Johnsgaard

Supervisor: Tor Einar Berg

Tor Einar Berg
Professor II

# Preface

This report is the result of my master thesis work spring 2010, at the Norwegian University of Science and Technology, NTNU and is the final step to complete my 5 year education to become Master of Science. The topic of this thesis is to reduce the complex lowering operation of the SCS through the sea surface to a simplified model for use as a design basis. This simplified model is then used to simulate the lowering operation in the time domain program SIMO. A model test setup of the same operation is suggested. To actually perform a model test is not a part of this thesis.

The work was initiated autumn 2009 in the form of a project thesis after suggestion by department manager analyses and engineering Helge Johnsgard [Johnsgard 10] at AMC located at Fornebu. The project thesis covered the static analysis of the lowering operation of the SCS along with an investigation into the compressibility of air and how to model this effect correctly in a geometrical scaled down model of the SCS.

During autumn 2009 and spring 2010 the project and later master thesis was developed and refined in cooperation with Stefan Schlömilch [Schlömilch 10] and Helge Johnsgards from AMC along with professor II Tor Einar Berg [Berg 10]. Tor Einar Berg was the supervisor both on the project and the master thesis.

The software program SIMO developed at MARINTEK is a difficult program to get started with as correct physical modeling and not the pedagogic layout is the main focus. Many hours was spent on understanding what SIMO requires, what it does with this information, and how to treat error messages.

A time costly lesson was learned with modeling in SIMO. Never start with a complicated model where one has no way of checking if the answer is correct, but rather start with an over simplified model that one fully understand and slowly expand this model to include new and more accurate physical effects.

I would like to thank Stefan Schlömilch and Helge Johnsgards from AMC for providing me with an interesting conceptual marine operation method for me to use in my project and master thesis and always finding time to help me with inputs and feedbacks on my assumptions and results from the analysis.

Thanks to Erik Lehn [Lehn 10], Knut Mo [Mo 10] and Peter Christian Sandvik [Sandvik 10] at MARINTEK for sharing their vast experience with planning and performing offshore model tests in the Ocean Basin and for their invaluable guiding and advising with the software program SIMO.

Finally, I would like to thank professor II Tor Einar Berg for being my supervisor for both the project and master thesis. His advices and network at MARINTEK proved very helpful.

Trondheim 14.06.2010

________________________________________

Henrik Kvadsheim

# Contents

X

## Nomenclature

| | | |
|---|---|---|
| $A, A_{ii}$ | Added mass | *Various* |
| $A_{load}$ | First order wave load amplitude | $[N]$ |
| $A_{SA}$ | Internal SA surface | $[m^2]$ |
| $A_{Trapped}$ | Trapped added mass | $[kg]$ |
| $A(ka)$ | Factor found from table | [-] |
| $A(\omega)$ | Frequency dependent added mass | *Various* |
| $a_S$ | Water particle acceleration | $[m/s^2]$ |
| $B_B$ | Beam barge | $[m]$ |
| $B_{SCS}$ | Beam SCS | $[m]$ |
| $BM_B$ | Initial meta centric height of barge | $[m]$ |
| $B_{55}$ | Damping in roll | $[kg/s]$ |
| $C, C_1, C_2$ | Stiffness | *Various* |
| $C_A$ | Added mass coefficient | [-] |
| $C_{corr,SA}$ | Correction coefficient | [-] |
| $C_l$ | Linear drag coefficient | [-] |
| $C_q$ | Quadratic drag coefficient | [-] |
| $c_p$ | Specific heat, constant pressure | $[J/gK]$ |
| $c_v$ | Specific heat, constant volume | $[J/gK]$ |
| $C_{55}$ | Roll stiffness | $[Nm/rad]$ |
| $d$ | Local depth | $[m]$ |
| $dF$ | Wave force on a small strip | $[N/m]$ |
| $dH_P$ | Change in differential head between two water levels | $[m]$ |
| $D_1, D_2$ | Damping | $[kg/s]$ |
| $f(\dot{x})$ | Vector function | *Various* |
| $F_{Buoyancy}$ | Buoyancy force from trapped air in SA | $[N]$ |
| $F_{water\ surf}$ | Pressure force acting on water surface inside SA | $[N]$ |
| $F_{waveload,amp}$ | Total first order wave force amplitude | $[N]$ |
| $F_{wire}$ | Load in wire | $[tonne]$ |
| $g$ | Gravity acceleration constant | $[m/s^2]$ |
| $GM_B$ | Transverse metacentric height for barge | $[m]$ |
| $H$ | Wave height | $[m]$ |
| $H(t)$ | Enthalpy, function of temperature only | $[J]$ |
| $H_B$ | Height of barge | $[m]$ |
| $H_{Disp\ water}$ | Differential head of displaced water | $[m]$ |
| $H_{Heave}$ | Forced vertical displacement of SA | $[m]$ |
| $H_S$ | Significant wave height | $[m]$ |
| $H_{SA}$ | Height of SA | $[m]$ |
| $H_{SCS}$ | Height of SCS | $[m]$ |
| $H_{Static}$ | Static water height | $[m]$ |
| $H_{0P}, H_1, H_{1P}$ | Differential head between two water levels | $[m]$ |
| $H_2, H_{2P}$ | Differential head between two water levels | $[m]$ |
| $H_6, \ldots, H_{22}$ | Submerged depth of SA | $[m]$ |
| $i$ | Various numbering | [-] |
| $I_{55,B}$ | Moment of inertia in roll for a barge | $[tonne \cdot m]$ |
| $k$ | Wave number | $[rad/m]$ |
| $k_{Axial}$ | Effective axial stiffness | $[N/m]$ |
| $K(x)$ | Hydrostatic stiffness | *Various* |

| | | |
|---|---|---|
| $K_1, K_2$ | Spring stiffness | $[N/m]$ |
| $KB_B$ | Buoyancy height for barge | $[m]$ |
| $KG_B$ | Mass height for barge | $[m]$ |
| $L_B$ | Length barge | $[m]$ |
| $L_{SCS}$ | Length SCS | $[m]$ |
| $m, m_h$ | Mass | $[kg]$ |
| $M, M_1, M_2$ | Mass | $[kg]$ |
| $P, P_1, P_{1P}, P_2, P_{2P}$ | Pressure | $[Pa]$ |
| $P_{atm}$ | Atmospheric pressure | $[Pa]$ |
| $P_{initial}$ | Initial Pressure | $[Pa]$ |
| $P_{winch}$ | Position of winches in x – and y-coordinate on the barges | $[m]$ |
| $q$ | External force | $[N]$ |
| $R$ | Universal gas constant | $[J/K]$ |
| $R_{SA}$ | Radius of a SA | $[m]$ |
| $R_{amp}$ | Amplitude of oscillation | $[m]$ |
| $t_{ms}$ | Time in model scale | $[s]$ |
| $t_{fs}$ | Time in full scale | $[s]$ |
| $t$ | Time | $[s]$ |
| $T$ | Temperature | [°C] |
| $T_d$ | Dampened eigenperiod | $[s]$ |
| $T_m$ | Wave period | $[s]$ |
| $T_{Max}$ | Maximum wire load allowed | $[tonne]$ |
| $T_{Min}$ | Minimum wire load allowed | $[tonne]$ |
| $U(T)$ | Internal energy, function of temperature only | $[J]$ |
| $U$ | Wind velocity at 10 m above sea level | $[m/s]$ |
| $u_s$ | Current flow | $[m/s]$ |
| $u(t)$ | Displacement as a function of time | $[m]$ |
| $V, V_{1P}, V_{2P}, V_R$ | Air volume | $[m^3]$ |
| $v_s$ | Submerged volume per unit length | $[m^2]$ |
| $V_{ms}$ | Volume model scale | $[m^3]$ |
| $V_{fs}$ | Volume full scale | $[m^3]$ |
| $V_{winch}$ | Release velocity of winch | $[m/s]$ |
| $W_{SCS,D}$ | Dry weight of SCS | $[tonne]$ |
| $W_{SCS,w}$ | Wet weight of SCS | $[tonne]$ |
| $x, \dot{x}, \ddot{x}$ | Displacement, velocity and acceleration vector | *Various* |
| $X$ | Fetch | $[km]$ |
| $\dot{x}_s$ | Strip velocity | $[m/s]$ |
| $X_{SCS}$ | Distance between center to center of SAs in x-direction | $[m]$ |
| $Y_{SCS}$ | Distance between center to center of SAs in y-direction | $[m]$ |
| $Z_{SCS}, \ddot{Z}_{SCS}$ | Vertical displacement and acceleration of SCS | *Various* |

**Greek symbols**

| | | |
|---|---|---|
| $\varepsilon$ | Phase angle | $[rad]$ |
| $\zeta_A$ | Wave amplitude | $[m]$ |
| $\theta_B$ | Heel angle of barge | $[rad]$ |
| $\dot{\theta}_B$ | Heel angular velocity of barge | $[rad/s]$ |
| $\ddot{\theta}_B$ | Heel angular acceleration of barge | $[rad/s^2]$ |
| $\kappa$ | Specific heat ratio | [-] |

| | | |
|---|---|---|
| $\lambda$ | Scaling factor | [-] |
| | Wave length | $[m]$ |
| $\xi$ | Damping ratio | [-] |
| $\rho$ | Density of sea water | $[kg/m^3]$ |
| $\omega$ | Frequency | $[rad/s]$ |
| $\omega_0$ | Eigen frequency | $[rad/s]$ |
| $\omega_{0,air}$ | Eigen frequency in air | $[rad/s]$ |
| $\omega_{0,water}$ | Eigen frequency in water | $[rad/s]$ |
| $\omega_d$ | Dampened eigenfrequency | $[rad/s]$ |
| $\phi$ | Velocity potential | $[m^2/s]$ |

## Abbreviation list

| | |
|---|---|
| AMC | Aker Marine Contractors |
| DNV | Det Norske Veritas |
| HydroD | Graphic modeling program where WADAM is executed |
| MARINTEK | Norwegian Marine Technology Institute |
| NTNU | Norwegian University of Science and Technology |
| SA | Suction Anchor |
| SIMO | Time domain program Simulation of Marine Operations |
| SCS | Subsea Compression Station |
| WADAM | Hydrodynamic analysis software |

# 1 INTRODUCTION

## 1.1 Scope and objective

The Ormen Lange gas field located 120 [km] West-Northwest of Kristiansund is under continuously development and a compression station is planned to be installed sometime between 2013 and 2016. Several concepts are investigated, but one of the most promising is the SCS. If this concept is chosen, the installation of the SCS poses many challenges due to the size and weight of the SCS and the depth of the Ormen Lange field.
AMC has developed a unique method for lowering the SCS through the sea surface and further down. The method involves the use of trapped air inside the SAs in order to reduce the crane load capacity required. The compressibility of the trapped air however, means that this buoyancy force will not be constant but reduce as the SCS is lowered down. The change in buoyancy force is largest close to the sea surface.

To investigate how the compressibility of the trapped air affects the crane load, a time domain simulation of the operation in a software program such as SIMO may be performed. To simulate the operation is not straight forward, but it is possible to include the important physics in a SIMO model.

Such a complex operation may also require a model test to verify the SIMO simulation result or to complement and increase accuracy of the input to the SIMO model. To geometrically scale down the SCS creates a problem with the compressibility of air, as a geometrically scaled down volume of the trapped air will behave much too stiff compared to the full scale.

This thesis will address how to create a simplified model of the lowering operation of the SCS which includes the important physical effects. The operation will be modeled in SIMO and simulated. A model test of the same operation will be investigated and discussed, and the result from the SIMO simulation will be the basis for determining which part of the model test that should be or not be performed. To actually perform a model test is not a part of this thesis.

## 1.2 Contributions

When creating a model of the lowering operation of the SCS in SIMO, a deep understanding of how SIMO calculates the forces and moments are crucial. The modeling of trapped air inside the SAs requires a depth changing and time dependent linear spring gradient, which accounts for change in air pressure with depth and if air is added or released. At this stage this is not an option in SIMO. After much considerations and discussion with the developers of SIMO at MARINTEK, a satisfying compromise on how to model the air spring was found. If a simulation in SIMO requires modeling of air springs, the work presented in this thesis may be used.

## 1.3 The lowering operation of the SCS through the sea surface

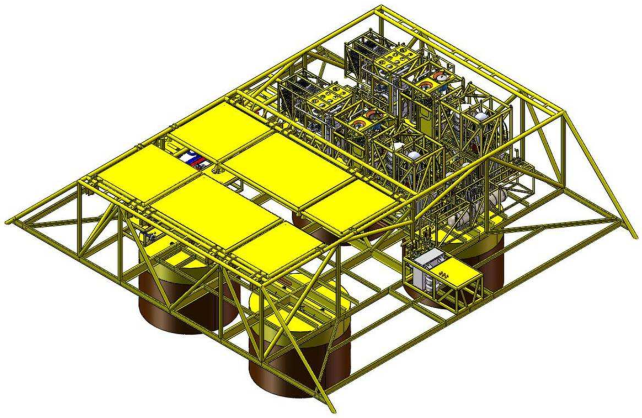

Figure 1 - Illustration of SCS

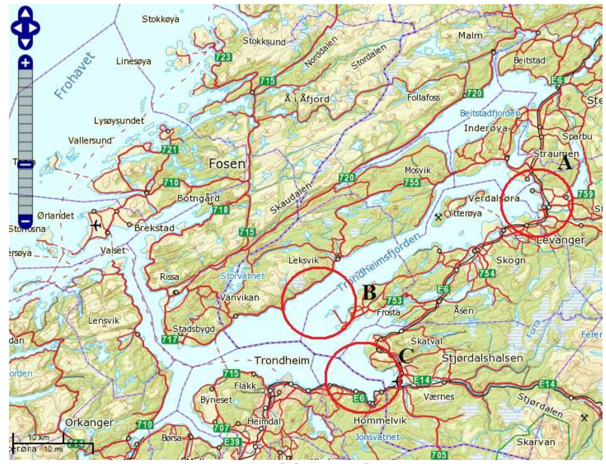



Figure 2 - Map of fjord of Trondheim

The SCS will, after completion and successful testing at Aker Verdal at location A in Figure 2, be skidded on to a semi submersible heavy lift vessel. After being transported past the shallow depth at location B to location C, the SCS is floated out from the semi submersible heavy lift vessel after the vessel has been sunk controllably. The SCS will now float on the trapped air inside the SAs. The trapped air provides more than adequate buoyancy force.

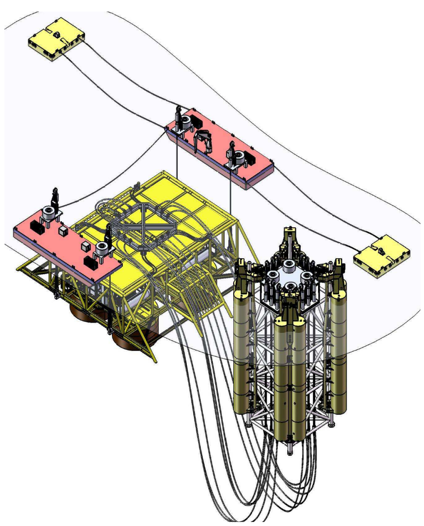

Figure 3 - The lowering operation of the SCS

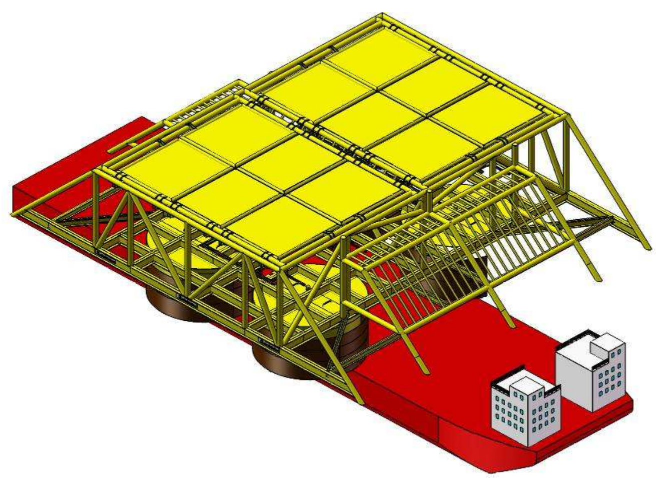

Figure 4 - SCS on semisubmersible heavy lift vessel

The floating SCS will now be held in place by tugs, and two North Sea barges will be positioned on opposite side. On each barge, two strand jack systems are installed and wire is feed through this system and connected to the SCS. The strand jacks will give the operators the control to slowly release wire. Four air compressors, two on each barge, will be connected by hoses to valves located on the top of each SA. This gives the operators the opportunity to release or to add air into the SAs. An illustration of the SCS when it has been lowered through the water is presented in Figure 5.

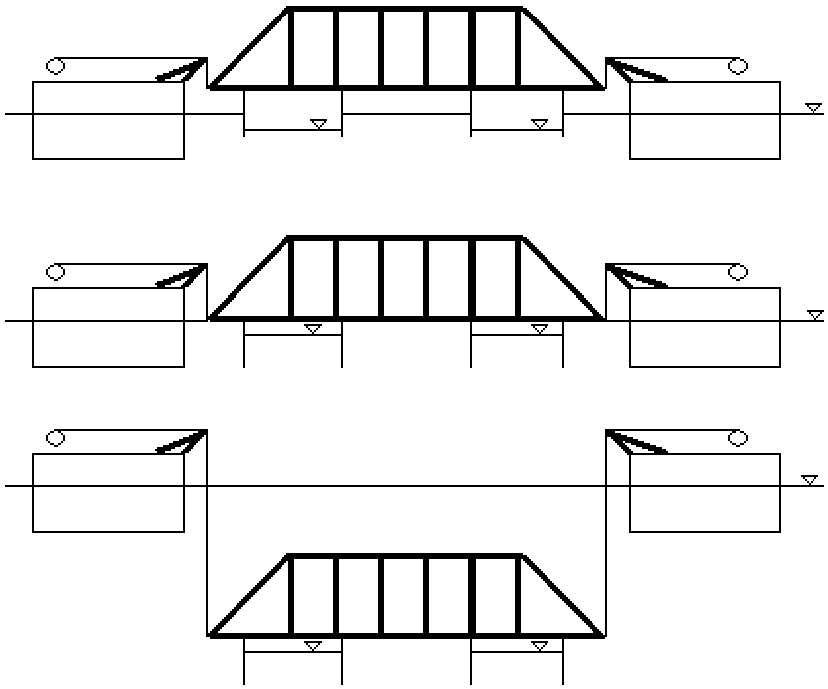

Figure 5 - Lowering operation of the SCS

The SCS is now floating on trapped air and connected to the two barges located on opposite side by four wires. Trapped air will now be slowly released from the SAs and the SCS starts to sink. As the SCS sinks lower, the tension in the wires starts to increase. The release of air is stopped when the tension reaches an upper limit in each wire. The next step is to release wire, and the SCS will sink further down. The tension will start to reduce, and the release of wire is stopped when the tension reads a determined lower limit. Next, air will be slowly released and so the operation sequence continues until the top of the SAs become submerged. The buoyancy force of the trapped air will now start to reduce as the SCS is lowered down by releasing wire, and the tension will start to increase. When the tension has reached the upper limit, compressed air must be added to reduce the tension down to the lower limit before more wire is released. This sequence is repeated until the SCS reaches a depth of $120$ $[m]$. The remaining operation until the SCS is installed on the Ormen Lange gas field is not relevant to this thesis and will therefore not be explained.

The most critical part of the lowering operation of the SCS is when the SAs goes from floating to submerged, because of the change of behavior of the trapped air. This will be one of the most important physical effects to include in the simplified model.

## 1.4 Organization of thesis

The layout of the thesis is organized into three main parts. First the general theory is presented. Second the design basis on which the time domain simulation will be modeled. Third and last, the SIMO model and simulation along with the simulation results and a discussion is presented along with a conclusion.

*Chapter 2* describes the theory of compressibility of air and model test, along with the software programs used and the SIMO theory.

*Chapter 3* states the design basis on which the time domain simulation is created from. Key dimensions, environmental conditions, simplified model of the lowering operation of the SCS, added mass calculation and compressibility of air spring calculation are covered by this chapter.

*Chapter 4* explains the SIMO model and the SIMO simulation of the lowering operation of the SCS.

*Chapter 5* presents and discusses the result from the SIMO simulation.

*Chapter 6* presents the conclusion and further work.

**The scope of work defined in the work description is answered in the following chapters**

| Scope of work # | Chapter |
|---|---|
| **1.** | Chapter 1.3 |
| **2.** | Chapter 2.1, 3.3 |
| **3.** | Chapter 2.2.3 – 2.2.4 |
| **4.** | Chapter 3.1 |
| **5.** | Chapter 3 |
| **6.** | Chapter 4 |
| **7.** | Chapter 5 |

Table 1 - Scope of work

## 1.5 Published literature

Several literature studies were performed during the thesis. Mostly the searches were conducted on Google Scholar [Google Scholar], and a large number of the relevant articles were available for viewing as long as the search was conducted through the NTNU network. A small number of articles could however not be viewed and the staff at the Library at Tyholt NTNU were very helpful by retrieving copies of these articles from paper editions kept in the Library storage at Tyholt and Hovedbygningen NTNU. Only the most relevant articles are mentioned. All the relevant articles are located in (Chapter A.8).

There had been some work done previously on similar operations using open bottom cans to add buoyancy to reduce draft for a gravity based structure towed over a shallow seabed. [Chakrabarti 94] and [Chakrabarti 95]. Should a model test of the part of the operation where the SCS is lowered through the water surface and down be necessary, much of the work done by Chakrabarti could be used.

When predicting the significant wave height with limited fetch a large number of articles was found. The two most relevant were [Carter 82] and [Erwing 80] which both discusses how to estimate significant wave height with limited fetch based on wave and wind measurements.

# 2 Theory

## 2.1 Compressibility of air

### 2.1.1 Introduction

To reduce the load on the lifting equipment, trapped air inside the SA will be used as additional buoyancy. A valve on each SA will give the operators the ability to release trapped air, and a compressor will give the ability to add air into the SAs. This is important because some trapped air must be released for the module to be able to sink when the SAs are floating. As the SAs becomes submerged, the hydrostatic pressure increases and compresses the gas. This will lead to decreased buoyancy and compressed air must be added to maintain trapped air volume to prevent too much of the SCS weight being transferred to the barges. The problem is largest close to the sea surface where the percentage absolute pressure change is the largest.

### 2.1.2 Ideal air

**Ideal gas and specific heat ratio, $\boldsymbol{k}$.**

The trapped air is assumed to obey the ideal gas model, because the internal energy of air at low density depends primarily on temperature. This gives the ideal gas model [Moran & Shapiro 06, pp. 100-104].

$$h(t) = u(T) + RT \tag{2.1}$$

Hence the specific heat is defined as a function of temperature alone:

$$C_v(T) = \frac{du}{dT} \tag{2.2}$$

Similarly, the specific enthalpy depends also only on temperature, and hence the specific heat is defined as:

$$C_{\text{p}}(T) = \frac{dh}{dT} \tag{2.3}$$

By inserting (2.2) and (2.3) in (3.1), one can obtain the specific heat ratio, $\kappa$, for an ideal gas.

$$\kappa = \frac{C_p(T)}{C_v} \tag{2.4}$$

**Polytropic process of an ideal gas**

A polytropic process is described by a pressure-volume relationship [Moran & Shapiro 06, pp. 112-113].

$$pV^n = Constant \tag{2.5}$$

Where n is a constant, and dependent on the particular process. For a polytropic process between two states

$$p_1V_1^{\ n} = p_2V_2^{\ n} \tag{2.6}$$

### Adiabatic process
For an isentropic process the specific heat is constant, $\Delta S = constant$, and hence no heat is transferred to or from the system. It can be showed that this corresponds to $n = \kappa$ where $\kappa$ can be found in [Moran & Shapiro 06, p. 754].

### Isothermal process
For an isothermal process the temperature is constant, $\Delta T = constant$, and heat is transferred to or from the system. It can be showed that this corresponds to n = 1.

### Actual process in the compressed air inside the SAs
The operation is planned to take place in the fjord of Trondheim during the summer, and so the temperature of the water at the surface is assumed to be somewhere between $10^{\circ}C$ and $20^{\circ}C$. Deeper down the temperature is assumed to be between $4^{\circ}C$ to $10^{\circ}C$.

The air inside the SAs will have contact with two types of surfaces; water and steel. The specific heat transfer coefficients for steel and water as a function of air pressure and air temperature has not been found, but all the coefficients that were found tended to be in order of 10-100 times larger for water than for steel. The trapped air is exposed to a steel area of $\pi R_{SA}^2 + 2\pi R_{SA} \cdot H_1$ and to a water area of $\pi R_{SA}^2$. Since water transfer heat so much more efficiently than steel, the water plane will be the dominant heat sink for the compressed air. This has been confirmed by Professor Harald Valland from Department of Marine Technology [Valland 09] and Associate Professor Reidar Kristoffersen from Department of Energy and Process Engineering [Kristoffersen 09].

When ideal air is assumed, the air can behave in two ways. An adiabatic process where no heat is transfer from or to the system or an isotherm process where the temperature is constant and the same as the water temperature. The dry weight of the module is very high, and hence the speed of the lowering operation will be very slow. Compressed air must also be pumped into the SAs as the trapped air pressure increases, to keep the buoyancy force from changing too much. AMC indicated a lowering speed of 20 [m/h] as an estimate. This slow lowering speed indicates that the heat buildup in the trapped air will have time to be transferred into the water due to the high heat transfer coefficient, and so will the trapped air behave as an isothermal process.

### Compressor
To keep the buoyancy force close to constant as the SCS is lowered down, compressed air must be added to the SAs. As the air is compressed by the compressor, the temperature of the air is increased. Hence this air contributes to a temperature increase of the air inside the SAs, but this temperature rise is very small due to the volume of the trapped air and the efficient cooling to the water surface.

## 2.2 Model test
The use of air filled SAs on a subsea structure is normally not a preferred installation method, and so the experience with this type of operation is limited. The results from the time domain simulation may need to be verified or the time domain simulation model may need complimentary or more accurate input. This may be achieved by a model test. The following chapter will explain how to correctly scale down the compressibility of air effect, suggest a setup of the model test of the lowering operation of the SCS along

with an example of modeling difficulty and describe how to find the hydrodynamic forces on the SCS along with an example on model dimensions.

### 2.2.1 Scaling

The Ocean Basin run by MARINTEK in Trondheim, Norway, is capable of handling test of offshore structure and marine operations, normally to a scaling factor of $\lambda=30 \rightarrow 60$.

### 2.2.2 Scaling of trapped air

The trapped air inside the SAs must also be scaled down. The air is assumed to follow the polytropic ideal air gas law (Eq. 2.6), but this poses well known problem. The volume of the air is correctly scaled down because the model is geometrically scaled down. The atmospheric pressure however cannot be scaled down unless the test facility can lower the air pressure, which is normally hard to accomplish and not done. So the atmospheric pressure is kept. Hence the volume needs to be adjusted in order to keep the polytropic relationship true.

Lets us consider a prototype can of unit cross sectional area and small thickness initially submerged in position 1. The internal pressure, $P_{1p}$, corresponds to a differential head, $H_{0p} + H_{1p}$, between the water level inside and the surface.[Chakrabarti 94, pp. 324-333]
If $P_{atm}$ represents the atmospheric pressure, then

$$P_{1p} = P_{atm} + H_{0p} + H_{1p} \tag{2.7}$$

and the air volume in the can is $V_{1p}$,

$$V_{1p} = H_{1p} \tag{2.8}$$

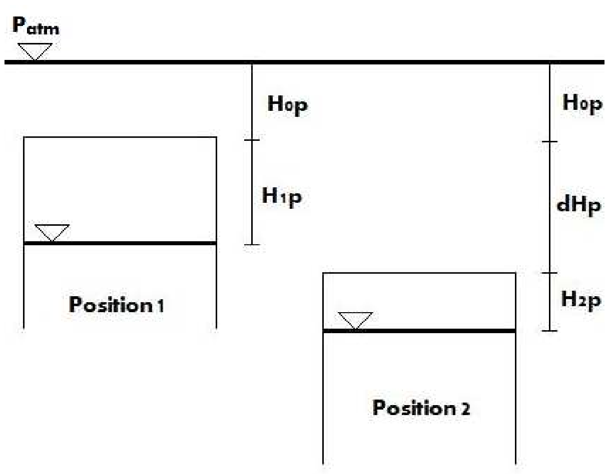


Figure 6 - Modeling of an open botton can

The volume is normalized by the cross area of the cans.
For the can in position 2, then

$$P_{2p} = P_{atm} + H_{0p} + dH_{p} + H_{2p} \tag{2.9}$$

and the air volume in the can is now $V_{2p}$,

$$V_{2p} = H_{2p} \tag{2.10}$$

Assuming that the relationship $PV^n$ is constant with n = 1 between position 1 and 2,

$$\left(P_{atm} + H_{0p} + H_{1p}\right)\left(H_{1p}\right) = \left(P_{atm} + H_{0p} + dH_{p} + H_{2p}\right)(H_{2p}) \tag{2.11}$$

When the can is modeled with a scale factor of $\lambda$, the gas law gives us

$$\left(P_{atm} + \frac{H_{0p}}{\lambda} + \frac{H_{1p}}{\lambda}\right)\left(\frac{H_{1p}}{\lambda}\right) = \left(P_{atm} + \frac{H_{0p}}{\lambda} + \frac{dH_{p}}{\lambda} + \frac{H_{2p}}{\lambda}\right)\left(\frac{H_{2p}}{\lambda} + V_{r}\right) \tag{2.12}$$

Where $V_r$ is the volume of air that must be added to the can volume to compensate for the fact that $P_{atm}$ will not be scaled in model size. Solving for the added volume, we get

$$V_r = \frac{\left(P_{atm} + \frac{H_{0p}}{\lambda} + \frac{H_{1p}}{\lambda}\right)\left(\frac{H_{1p}}{\lambda}\right)}{\left(P_{atm} + \frac{H_{0p}}{\lambda} + \frac{dH_{p}}{\lambda} + \frac{H_{2p}}{\lambda}\right)} - \frac{H_{2p}}{\lambda} \tag{2.13}$$

### Modeling of compressed air with an external air tank

The setup of a model test requires an additional volume of air if the compressed air should be modeled correctly. This volume, $V_r$ , must be stored outside the model, hence an external air tank is used. The flexible hose that connects the added air tank to the model must not influence the flow around the model or introduce forces into the model.

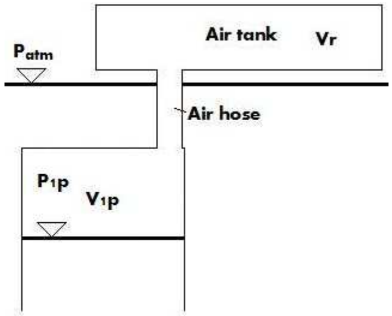


Figure 7 - Added air volume setup

To figure out the dimension of the hose, the maximum volume flow is assumed. The connection between the volumes and time in model scale and full scale is as follows

$$t_{ms} = \frac{t_{fs}}{\sqrt{\lambda}} \quad (2.14)$$

$$V_{ms} = \frac{V_{fs}}{\lambda^3} \quad (2.15)$$

### Modeling of the compressed air by using a membrane

A different way of modeling the properties of the trapped air is by using a membrane as shown in Figure 8. Springs can be fitted to the top of the SAs, and by quasi static approach the dynamic properties heave motion can be examined. The springs must be designed for a given depth, so the result will only be accurate close to the design depth.

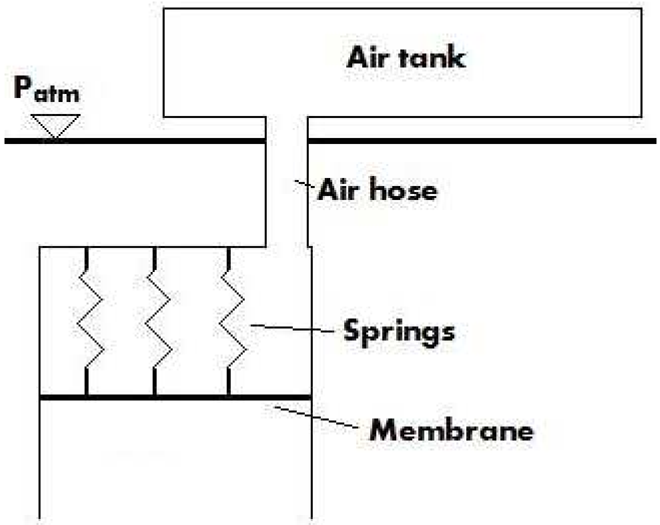


Figure 8 - Spring supported membrane setup

The membrane would need to be water tight to keep water from leaking in to the air section, but this membrane has its own damping, stiffness and eigenfrequency, which may introduce unwanted influence in to the result. As the membrane is displaced, the volume of air must also be displaced, so the challenge with added air is not solved by use of a membrane.

## 2.2.3 Model test setup of the lowering operation of the SCS

The lowering operation of the SCS through the sea surface is one of the critical parts of the operation to transport the SCS from the construction site to final installation site at Ormen Lange. The reason is the change of how the trapped air behaves with respect to buoyancy as the SAs goes from a floating position to a submerged position. For the compressibility of air effect to be included in the geometrical scaled down model test, external air tank must be added.

### Model test setup suggestion

To model the lowering operation of the SCS through the Sea surface, a geometrical scaled down model of the SCS with external air tanks connected is used. This will capture the correct scaled down depth dependent compression of air effect requires a correct modeling of the trapped air. The two barges can be represented by four springs and four electrical motors. One spring will represent half the heel stiffness of one barge. The larger the tension in the wires becomes, the more the springs extend which corresponds to larger barge heel. One electric motor represents one of the two strand jack systems onboard each barge, and is used to release wire.

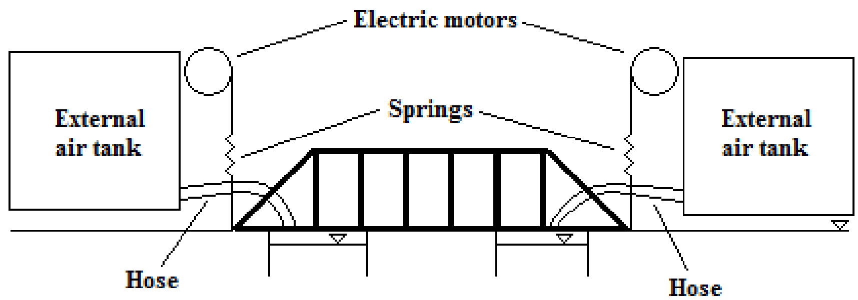


**Figure 9 - Suggestion of model setup for the lowering operation of the SCS**

After discussing this setup of the model of the lowering operation with Erik Lehn [Lehn 10] and Peter Sandvik [Sandvik 10] at MARINTEK which have vast experience with offshore model testing, they did not recommend this setup. The electric motors introduce some unwanted damping, but the show stopper is the modeling of trapped air by the use of external air tanks. The flexible hoses connecting the SAs to the air tanks will be to stiff and affect the motion of the SCS model considerably. However, the correct modeling of the compressibility of air is the important key part of the model test. So the suggested model setup is not a god solution, and no alternative solutions on how to include the correct compressibility of air effect in a geometrical scaled down model of the SCS has been found. The following example which shows unwanted viscous damping caused by the flow of air through the hoses connecting the trapped air to the external air tanks, illustrates one of the problems with the modeling setup.

### Example

This example is intended to show one of the challenges of using external air tanks in a model scale. The challenge is unwanted viscous damping of air flowing through the hoses, and how the challenge increases with decreasing model size.

A full scale can is assumed to have a diameter of 20 $[m]$ and a height of 12 $[m]$. The top of the can is just below sea level and the can has a buoyancy force equal to 1000 $[tonne]$. The can moves downwards 1 [m] in 60 [s], no air is released or added. The air follows isotherm ideal gas law, and the surface pressure is standard pressure at 20 [deg]. Key values for 3 different scaled down models is showed in Table 2 and are calculated with (Chapter A.3) [White 05, pp. 24,361-362] [Steen & Aarsnes 08, p. 11]

| Scale | λ = 30 | λ = 45 | λ = 60 | Dimension |
|---|---|---|---|---|
| **Volume of trapped air in one SA** | 36.1 | 10.7 | 4.5 | $[Liter]$ |
| **Added air volume** | 315.0 | 145.1 | 83.0 | $[Liter]$ |
| **Fraction added air over trapped air** | 8.7 | 13.6 | 18.4 | $[-]$ |
| **Time** | 11.0 | 8.9 | 7.8 | $[s]$ |
| **Volume displaced** | 2.1131 | 0.62612 | 0.26414 | $[Liter]$ |
| **Volume flow** | 0.1929 | 0.07000 | 0.03410 | $[\frac{Liter}{s}]$ |
| **Overpressure** | 1015.5 | 677.0 | 507.7 | $[Pa]$ |
| **Pressure drop, D =0.05 m hose** | 0.008626 | 0.0014636 | 0.00041572 | $[Pa]$ |
| **Pressure drop, D =0.01 m hose** | 18.0268 | 3.05857 | 0.868784 | $[Pa]$ |

Table 2 - Model scaling ratio key values

The pressure drop from the 1 [m] of hose is low for a 5 [cm] diameter hose, but very high for a 1 [cm] diameter hose. The problem is that a 5 [cm] diameter hose would be very impractical to use in the three model sizes due to the size of the hose is so large compared to the models. The pressure drop in the hose will give unwanted viscous damping to the dynamic system, hence should it be kept as low as possible.

### 2.2.4 Model test of the hydrodynamic forces on the SCS

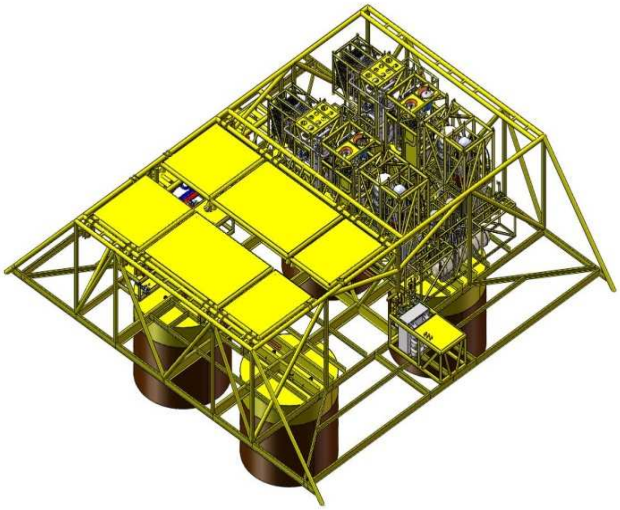

The SCS module consists of a very complex geometry structure along with four compressor trains and four SAs. The hydrodynamic forces are due to the complexity not easy to predict, and if the time domain simulation of the lowering operation of the SCS shows that dynamics play a vital role, a model test to more accurately determine the hydrodynamic forces input to the time domain model may be needed.

#### Added mass and damping from potential theory

The hydrodynamic loads are added mass and damping loads on the SCS, which are steady state forces and moments due to forced harmonic rigid body motion. The outgoing waves are not a result of the incident waves but the forced motion of the SCS results in oscillating fluid pressures over the SCS surface.

Integration of the fluid pressure forces over the body surface gives resulting forces and moment on the SCS. These outgoing waves transport energy away from the oscillating SCS and so acts as a damping. The shape of the SCS, the frequency of the oscillation, the depth of the SCS, the lowering speed of the SCS, finite water depth and restricted water are important with respect to the added mass and the damping. [Faltinsen 09]

### Determining added mass and damping through a model test

To determine the added mass and damping of the geometrical scaled down model, a decay test may be performed. The model is attached to a rig, where it is connected to a linear spring. First the eigenperiod in air of the model is found. The model is displaced a known distance, and released. The oscillations as a function of time is then measured, and analyzed to find the eigenperiod $\omega_{0,air}$.

$$\omega_{0,air}^2 = \frac{C}{M} \tag{2.16}$$

where C is the spring stiffness and M is the mass of the SCS model.
The model is lowered into water and the same test is performed again to find the new eigenperiod. The model is displaced a known distance and released. The oscillations as a function of time is then measured, and analyzed to find the eigenperiod $\omega_{0,water}$.

$$\omega_{0,water}^2 = \frac{C}{M + A} \tag{2.17}$$

Solving both (Eq. 2.16) and (Eq. 2.17) for stiffness $C$ and setting them equal to each other

$$\omega_{0,water}^2 (M + A) = \omega_{0,air}^2 M \tag{2.18}$$

And solving for the added mass $A$

$$A = M \left[ \left( \frac{\omega_{0,air}}{\omega_{0,water}} \right)^2 - 1 \right] \tag{2.19}$$

The damping of the SCS is found by assuming that the oscillations follow $u(t)$.

$$u(t) = e^{-\xi \omega_0 t} R_A \cos(\omega_d t + \epsilon) \tag{2.20}$$

$\omega_d$ is the dampened natural frequency, given by

$$\omega_d = \sqrt{1 - \xi^2} \tag{2.21}$$

The relation between the damped frequency and damped period is $T_d = 2\pi/\omega_d$
An expression for the damping ratio is achieved by deriving the relation between two maxima ($i$ and $i+n$). The damping ratio is assumed to be small so that $\sqrt{1-\xi^2} \approx 1$.

$$\frac{u_i}{u_{i+n}} = \frac{u(t_i)}{u(t_i+nT_d)} = \frac{e^{-\xi\omega_0 t_i} R_A \cos(\omega_d t_i + \epsilon)}{e^{-\xi\omega_0(t_i+nT_d)} R_A \cos(\omega_d(t_i+nT_d)+\epsilon)} = \frac{e^{-\xi\omega_0 t_i}}{e^{-\xi\omega_0(t_i+nT_d)}} = e^{\xi\omega_0 nT_d} \quad (2.22)$$

$$\xi\omega_0 T_d = \xi\frac{\omega_d}{\sqrt{1-\xi^2}} T_d = \frac{2\pi\xi}{\sqrt{1-\xi^2}} \approx 2\pi\xi \quad (2.23)$$

$$\xi = \frac{1}{2\pi n} ln\left(\frac{u_i}{u_{i+n}}\right) \quad (2.24)$$

Two maxima, at the time $t_i$and $t_i + T_d$, and the number of oscillations between them, n, must be gathered from a plot of the oscillations.

### Model test setup suggestion

To determine the added mass and damping of the SCS a decay test of the geometrical scaled down model of the SCS may be performed. However, the compressibility of air will not be correctly scaled as the scaled down air volume means that the air will behave much too stiff. The use of external air tank as discussed in (Chapter 2.2.2) will introduce unwanted and false damping and stiffness to the model due to the flexible hoses, so external air tanks cannot be used.

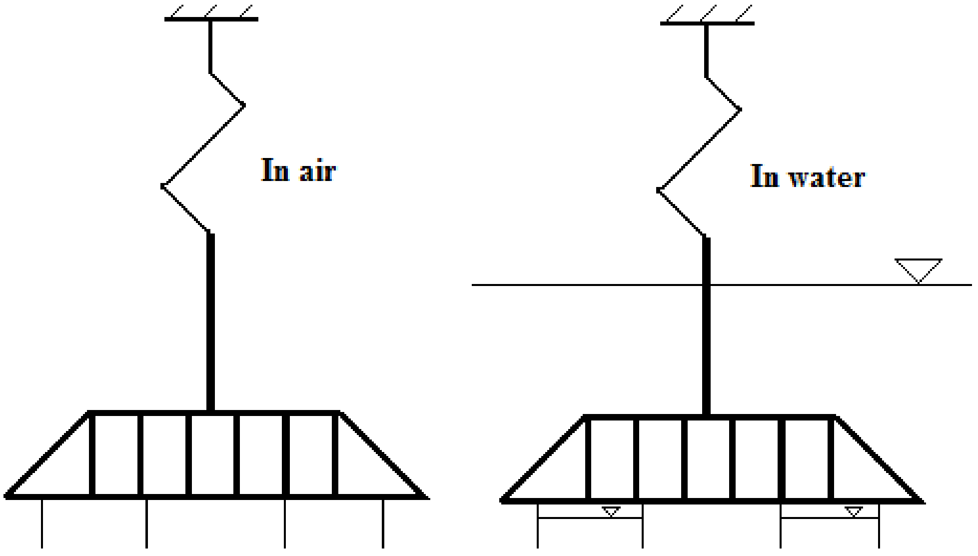


Figure 10 - Decay setup of SCS model

The magnitude of the added mass inside and underneath the SAs will probably not change dramatically if the trapped air is not modeled correctly, but the phase difference may be interesting.
A solution would then be to model one SA alone, and instead of trying to connect the trapped air to an

external air tank by a hose, one can simply modify the SA by extending it upwards and so increase the volume to the correct amount.

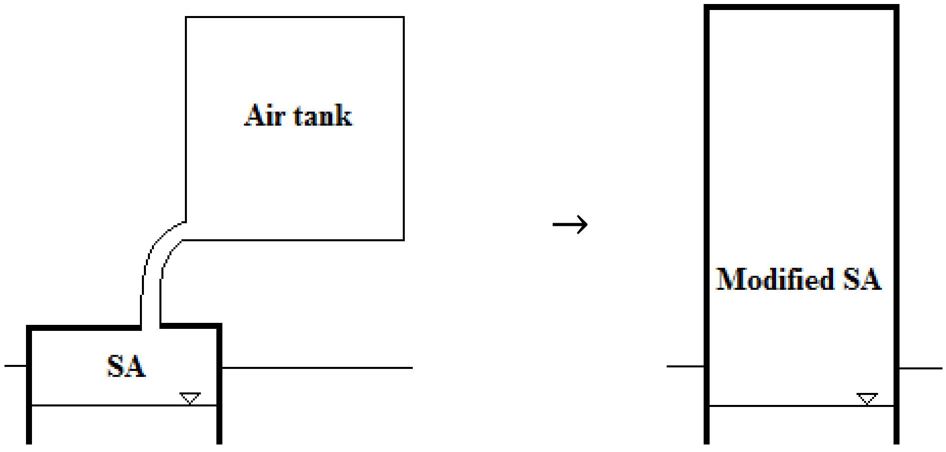


Figure 11 - Modeling of SA with correct compressibility of air effect

### Example

To get a physical understanding on how large such a modified SA could be, the same three scaling ratios $\lambda = 30, 45$ and 60 are chosen.

| Scale | $\lambda = 30$ | $\lambda = 45$ | $\lambda = 60$ | Unit |
|---|---|---|---|---|
| **Volume of trapped air in one suction anchor** | 54.2 | 16.1 | 6.8 | $[Liter]$ |
| **Added air volume** | 297.6 | 139.9 | 80.8 | $[Liter]$ |
| **Fraction added air over trapped air** | 5.5 | 8.7 | 11.9 | $[-]$ |
| **Diameter of geometrical scaled model of SA** | 0.67 | 0.44 | 0.33 | *[m]* |
| **Height of geometrical scaled model of SA** | 0.40 | 0.27 | 0.2 | *[m]* |
| **Added air volume divided by $A_{SA}$ of model** | 0.85 | 0.90 | 0.93 | *[m]* |
| **Height of modified model of SA** | 1.25 | 1.17 | 1.13 | *[m]* |
| **Fraction height modified model over diameter geometrical scaled model of SA** | 1.87 | 2.66 | 3.42 | *[-]* |

Table 3 - Example of modified SA

The correct modeling of trapped air inside a SA by modifying the height of the SA is fully possible, and should give clear results. The difference between the three scaling rations is not very large and of no importance with regards to test results, so the smallest model could be preferred because it is the easiest to build and handle in the test rig. If for some reason the amount of trapped air should be reduced, one can simply attach a cylinder of very light and stiff foam inside the top of the model of the SA and so reducing the air volume. An interesting problem would be to reduce the trapped air volume in the model systematically, but keeping the water level inside the SA and find the added mass and damping. This would establish if correct modeling of the trapped air is important with respect to added mass and damping. One important notice must be taken, the model test of a modified SA is a two mass dynamic system.

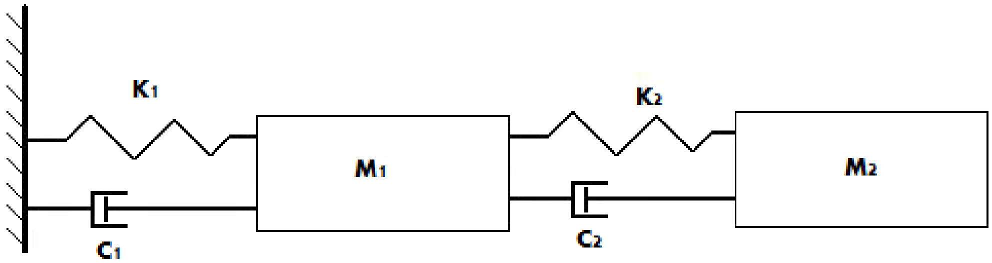


Figure 12 - Illustration of a two mass dynamic system

where

| | |
|---|---|
| M1 | Mass of SA |
| M2 | Added mass inside and underneath the SA |
| K1 | Linear spring |
| K2 | Trapped air spring |
| C1 | Damping |
| C2 | Damping |

## 2.3 Description of Software

To simulate the lowering operation of the SCS through the surface in time domain, the time domain simulation program SIMO was used. Due to modeling difficulties of wave forces on the SAs, the resulting first order wave force amplitude found from SIMO, was compared with the resulting first order wave force amplitude found from hydrodynamic analyze software WADAM and hand calculations. The goal was to be able to model the first order wave forces on the SAs in the SIMO model correct using slender elements. This chapter will give an overview of the software tools SIMO and WADAM.

### 2.3.1 SIMO

SIMO is a time domain simulation program for multi-body systems allowing non-linear effects to be included in the wave-frequency range. Flexible modeling of station-keeping forces and connecting force mechanisms (anchor lines, ropes, thrusters) is included.
The results from the program are presented as time traces, statistics and spectral analysis of all forces and motions of all bodies in the analyzed system. It is a modular and interactive computer program with batch processing options. Typical applications include TLP installations, offshore crane operations, floating production systems and dynamic positioning systems. [SIMO user manual]

SIMO is divided into 6 separate modules. In addition to these, a 3D visualization program SimVis, exists.

INPMOD - Input data manipulation
STAMOD – Initial condition and static equilibrium
DYNMOD – dynamic response calculations
OUTMOD – output module

S2XMOD – export of time series
PLOMOD – plotting module
SimVis - visualization

Different kinds of files are needed to run SIMO. Definition of body types, coupling and environmental data is described in the system description file, SYSFIL. The SYSFIL is read by STAMOD and an initial condition file INIFIL is generated. The INIFIL contains a complete system description where the environment and initial positions is defined. DYNMOD utilizes the INIFIL to execute the time domain simulation. Both STAMOD and DYNMOD can write visualization files VISFIL to SimVis. Post-processing or export of results is done by OUTMOD or S2XMOD. Graphic presentation of the results is possible using PLOMOD where the DYNMOD generated plotting files PLOFIL is read.

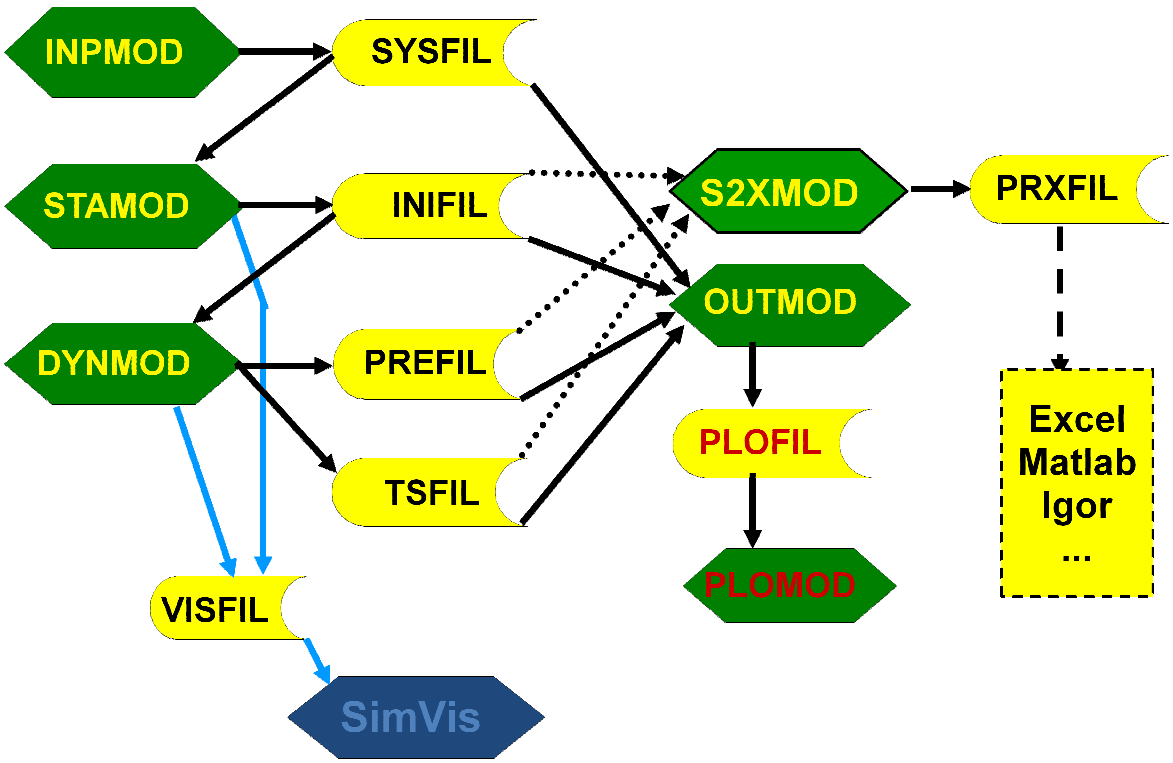


Figure 13 - Program flow in SIMO

### INPMOD- input data manipulation

The purpose of the module is to read and manipulate input from external data sources, for example hydrodynamic programs, and to modify the system description file, SYSFIL.

### STAMOD- initial condition and static equilibrium

Initial conditions for the system are needed to perform a dynamic simulation. STAMOD defines these by reading the SYSFIL and writes the INIFIL that contains the complete description of the system such as definition of the environment and the initial position. It is possible to modify the present system, e.g. specification of environment, positioning or restoring forces. Before writing the INIFIL, static equilibrium may be calculated which in turn updates the initial positions. A visualization file may be written which can be viewed in SimVis.

#### DYNMOD-dynamic response calculation
DYNMOD performs a time domain simulation of the system with initial conditions as defined by the INIFIL. Responses are calculated by starting a time integration of the equation of motion. Before the time domain simulation can start, main simulation parameters must be specified. A visualization file may be written which can be viewed in SimVis

#### OUTMOD- output module
OUTMOD presents results from the time domain simulation by generating print and plot of time series and statistical parameters created by DYNMOD.

#### S2XMOD-export of time series
S2XMOD presents results from the time domain simulation by generating export files to external programs in formats such as .m-files (MatLab), ASCII-files and DIRECT ACCESS-files. S2XMOD gives an overview of all series generated by SIMO and can also produce simple statistics and plot of these.

#### PLOMOD- plotting module
PLOMOD gives the possibility of generating an interactive real time 3-dimensional plot.

#### SimVis-3D visualization program
SimVis is a stand alone program based on GLView used to visualize the time domain simulation. A useful application of SimVis is the fact that modeling errors are more easily detected when the system is visualized. STAMOD is only capably of generating a static picture of the system, where DYNMOD creates the entire time domain simulation. The project file system, (filename.svp) contains the main input to SimVis such as body locations, which bodies are to be visualized, which geometry describes each body and description of the sea floor and ocean floor. All the bodies and couplings modeled in SIMO can be visualized. Coupling elements and slender elements are shown automatically, but the other geometries have to be visualized from geometry files or by defining simple body shapes in the project file.

### 2.3.2 WADAM
WADAM is a general hydrodynamic analysis software for calculating wave-structure interaction for fixed and floating structures of arbitrary shape. WADAM is based on widely accepted linear methods for marine hydrodynamics using the 3-D radiation-diffraction theory and employs a panel model (created in GeniE) and Morison equation in linearized form employing a beam model. WADAM is often executed from HydroD where graphic modeling of the environment is done.
GeniE is a tool for designing and analyzing offshore and maritime structures made of beams and plates. Modeling, analysis and results processing are performed in the same graphical user interface. For floating structures, GeniE can perform static and dynamic linear analysis for structures subjected to wave, wind, current, ballast and equipment layout. The loads and accelerations from the waves and compartment content are defined by HydroD and they are automatically applied to the structure model independent of the hydrodynamic panel model.

## 2.4 SIMO theory
The process of modeling the lowering operation of the SCS involves the time domain simulation program SIMO. SIMO requires different input parameters dependent on the body type chosen and which physical effects one wishes to include. To understand and check the results, it’s important to understand which assumptions are made, which formulas are used during the calculations and how SIMO uses these formulas.
SIMO’s main objective is to solve the equation of motion to find the load and response history given with respect to time.

### 2.4.1 Equation of motion

In a simplified form, the equation of motion for a system of one or several bodies may be written:

$$(\mathbf{m} + \mathbf{A}(\boldsymbol{\omega}))\ddot{\boldsymbol{x}} + \boldsymbol{C}\dot{\boldsymbol{x}} + \boldsymbol{D_1}\dot{\boldsymbol{x}} + \boldsymbol{D_2}\boldsymbol{f}(\dot{\boldsymbol{x}}) + \boldsymbol{K}(\boldsymbol{x})\boldsymbol{x} = \boldsymbol{q}(\boldsymbol{t}, \boldsymbol{x}, \dot{\boldsymbol{x}}) \tag{2.25}$$

where

$$\boldsymbol{q}(\boldsymbol{t}, \boldsymbol{x}, \dot{\boldsymbol{x}}) = \boldsymbol{q_{WI}} + \boldsymbol{q_{WA}^{(1)}} + \boldsymbol{q_{WA}^{(2)}} + \boldsymbol{q_{CU}} + \boldsymbol{q_{ext}} \tag{2.26}$$

and

| | |
|---|---|
| $\boldsymbol{m}$ | Body mass matrix |
| $\boldsymbol{A}(\boldsymbol{\omega})$ | Frequency dependent added mass |
| $\boldsymbol{C}$ | Frequency dependent potential damping matrix |
| $\boldsymbol{D_1}$ ***and*** $\boldsymbol{D_2}$ | Linear and quadratic damping matrix |
| $\boldsymbol{f}(\dot{\boldsymbol{x}})$ | Vector function where each element is given by $f_i = \dot{x}_i\lvert\dot{x}_i\rvert$ |
| $\boldsymbol{K}$ | Hydrostatic stiffness matrix |
| $\boldsymbol{x}, \dot{\boldsymbol{x}}, \ddot{\boldsymbol{x}}$ | Positioning, velocity and acceleration vector |
| $\boldsymbol{q_{WI}}$ | Wind drag force |
| $\boldsymbol{q_{WA}^{(1)}}$ | 1. order wave excitation force |
| $\boldsymbol{q_{WA}^{(2)}}$ | 2. order wave excitation force |
| $\boldsymbol{q_{CU}}$ | Current drag force |
| $\boldsymbol{q_{ext}}$ | Any other forces (wave drift damping, specific forces and forces from station-keeping and coupling elements, etc.) |

### 2.4.2 Modeling capabilities

#### Environmental forces

Wind, waves and current are important environmental forces that SIMO can include in the simulation. Several wind spectra, wind gust spectra and current profile can be modeled, together with regular and irregular wave spectra. The irregular wave spectra can be described by one and two parameter JONSWAP spectrum and the two-parameter Pieson-Moskowitz spectrum. Linear wave potential theory is used where the undisturbed, incoming wave field is determined by the wave potential, Φ, expressed by Airy's theory.

$$\Phi = \frac{\zeta_A g}{\omega}\frac{\cosh\big(k(z+d)\big)}{\cosh\,(\mathrm{kd})}\cos\,(\omega\mathrm{t} - \mathrm{kx}\cos\beta - \mathrm{ky}\sin\beta + \phi_{\zeta_A}) \tag{2.27}$$

where

| | |
|---|---|
| $\Phi$ | Velocity potential |
| $\zeta_A$ | Wave amplitude |
| $k$ | Wave number |
| $z$ | Specified depth |
| $d$ | Local depth |
| $\omega$ | Angular wave frequency |

#### Slender Elements

*Slender elements* can be used to model jacket legs and bracings or spool pieces. The modeled structure may consist of several slender elements, each given specific properties like hydrodynamic coefficients, rotation stiffness and mass data. Each element is divided into a specific number of strips of equal length where the induced forces are calculated on the middle of each strip. The external load on slender elements consists of buoyancy forces, wave forces and slamming forces. The result force on an element is the force contribution from each strip, and the total body force is the sum of contributions from all elements.

The buoyancy and gravity force acts in the global z-direction, through the center of buoyancy and gravity. The gravity and buoyancy load vectors for a strip, expressed in the global coordinate system:

$$F_{buoyancy} = \begin{bmatrix} 0 \\ 0 \\ \rho V_S g ds \end{bmatrix} \tag{2.28}$$

$$F_{Gravity} = \begin{bmatrix} 0 \\ 0 \\ -mgds \end{bmatrix} \tag{2.29}$$

The wave load vector for a strip, expressed in the local strip coordinate system:

$$\boldsymbol{F}_{W,S} = (\rho V_S + \boldsymbol{m}_h)\boldsymbol{a}_S + \boldsymbol{C}_q\{(\dot{\boldsymbol{X}}_S - \boldsymbol{U}_S - \boldsymbol{v}_S)|\dot{\boldsymbol{X}}_S - \boldsymbol{U}_S - \boldsymbol{v}_S|\} + \boldsymbol{C}_l(\dot{\boldsymbol{X}}_S - \boldsymbol{U}_S - \boldsymbol{v}_S) \tag{2.30}$$

where

| | |
|---|---|
| $V_S$ | Submerged volume per unit length, calculated to $z = 0$ |
| $\boldsymbol{m_h}$ | Hydrodynamic mass of the element |
| $\boldsymbol{a_S}$ | Water particle acceleration in local strip coordinate system |
| $\boldsymbol{C_q}$ | Quadratic drag coefficient |
| $\dot{\boldsymbol{X}}_{\boldsymbol{S}}$ | Strip velocity in local coordinate system |
| $\boldsymbol{U_S}$ | Current flow in local coordinate system |
| $\boldsymbol{v_S}$ | Water particle velocity in local strip coordinate system |
| $\boldsymbol{C}_l$ | Linear drag coefficient |

The first term contains the Froude-Krylov force and diffraction forces. The second term is the quadratic drag term of Morison's equation. The third term represents linear drag. A close observation of equation (Eq. 2.30) and the Froude-Krylov term show that if one do not want the buoyancy force from a slender element, one can simply set the submerged volume $V_S$ to zero and adjust the added mass $\boldsymbol{m_h}$ so the term $(\rho V_S + \boldsymbol{m}_h)$ remains constant. This is an important trick used in the SIMO model of the lowering operation of the SCS. The result is that the first order wave force remains constant but the buoyancy force becomes zero.

### Coupling points

*Coupling points* is used to define a point on a body where coupling forces can be attached. Specific properties such as a winch can be added to a coupling point, giving the user the ability to hoist in or out wire.

### Position system

The *fixed force elongation* positioning system may be used to hold a body in a mean position such as a moored barge in waves or to represent the buoyancy force of the trapped air inside the SAs on the SCS. As a coupling force, any force-elongation relationship may be specified. The curves for increasing and decreasing elongation may be different in order to model hysteresis effects. Damping may be specified as a force proportional to any exponent of the relative velocity of the end points. SIMO will interpolate between elongations to estimate the force.

#### Coupling forces

The forces acting on the lifting wires used in the lowering operation of the SCS are important aspects in load handling with regards to dimensioning and control. SIMO offers three main alternatives to represent the coupling forces, and only *simple wire coupling* is used in modeling of the lowering operation of the SCS. The simple wire coupling is modeled as a linear spring according to:

$$\Delta l = \frac{F_{wire} g}{k_{Axial}} \tag{2.31}$$

where

| | |
|---|---|
| $F_{wire}$ | Wire tension load |
| $k_{Axial}$ | Effective axial stiffness |

### 2.4.3 Solution

The equation of motion (Eq. 2.25) can finally be solved when the external forces have been determined and the structural mass and stiffness matrixes have been defined. For solving the equation, two approaches are used; solution by convolution integral or by separation of motions. The solution by convolution integral is used to find the harmonic output due to harmonic input with the impulse-response method. However, this is only of interest if a frequency dependent added mass or damping is modeled. The solution by separation of motions separates the exciting forces and position vectors into a high frequency interval and low frequency interval. The high frequency motions are solved in the frequency domain and the low frequency motions are solved in the time domain.

### 2.4.4 Numerical integration

To solve the equation of motion (Eq. 2.25) from time step to time step, numerical integration is used. By using the values on time step as initial values and assuming how the acceleration term will behave, the next time step can be approximated. These new values are then set to initial values, and so step by step an approximate solution is found for any given point of time. The accuracy is determined by several factors but the length of the time step is among the most important. SIMO offers three different methods when approximating how the acceleration is estimated over a time step:

1. *Modified Euler Method* where the initially acceleration is used as constant acceleration.
2. $3^{rd}$-*order Runga-Kutta-like method* where the average acceleration over one time step is used.
3. *Newmark $\beta$-Predictor-Corrector Method* where the $\beta$-value determines different types of accelerations.

# 3 Design basis

## 3.1 Key dimension

The dimensions and weight of the SCS is among the main motivations for using trapped air as buoyancy force to reduce the crane load. Only the dimensions of the SCS and a standard North Sea barge relevant for this thesis are included. As the SCS is still at the planning phase, changes to the dimension and weight should be expected. All the dimensions are provided by AMC and Aker Solutions.

### 3.1.1 Key values of the SCS

| Key figure | Value | Dimension |
|---|---|---|
| **Length $L_{SCS}$** | 74 | $[m]$ |
| **Beam $B_{SCS}$** | 80 | $[m]$ |
| **Height $H_{SCS}$** | 27 | $[m]$ |
| **Dry weight $W_{SCS,D}$** | 8000 | $[tonne]$ |
| **Wet weight $W_{SCS,w}$** | 6000 | $[tonne]$ |
| **Height of SA $H_{SA}$** | 12 | $[m]$ |
| **Radius of SA $R_{SA}$** | 10 | $[m]$ |
| **Internal water surface area of SA $A_{SA}$** | 314 | $[m^2]$ |
| **Distance from center to center of the SAs** | | |
| **X direction $X_{SCS}$** | 30 | $[m]$ |
| **Ydirection $Y_{SCS}$** | 50 | $[m]$ |

Table 4 - Key values of SCS

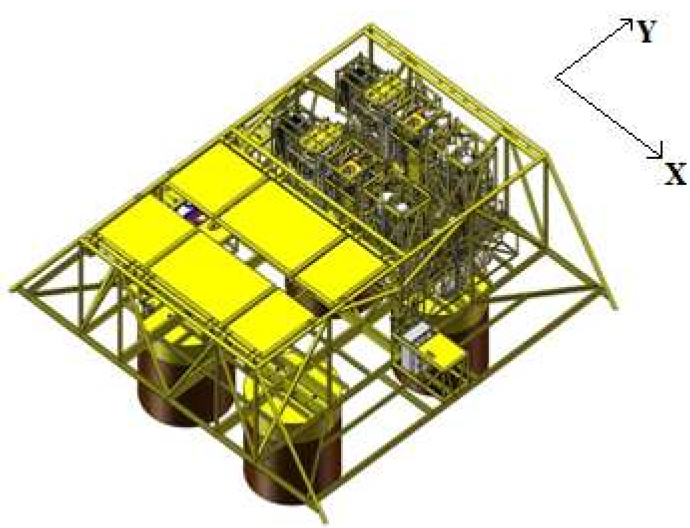


Figure 14 - SCS illustration

### 3.1.2 Key values a North Sea barge

| Key figure | Value | Dimension |
|---|---|---|
| **Length $L_B$** | 91.5 | $[m]$ |
| **Beam $B_B$** | 27.4 | $[m]$ |
| **Height $H_B$** | 6.1 | $[m]$ |
| **Moment of inertia in roll $I_{55,B}$** | 729991 | $[tonne \cdot m]$ |
| **Maximum tension in each wire $T_{max}$** | 500 | $[tonne]$ |
| **Minimum tension in each wire $T_{min}$** | 300 | $[tonne]$ |
| **Winch lowering speed $V_{Winch}$** | 20 | $[m/h]$ |
| **Coordinate of winches (x - , y - coordinates) $P_{Winch}$** | $(\pm 22, 13.7)$ | $[m]$ |

**Table 5 - Key values of a standard North Sea barge and pretension value**

## 3.2 Environmental conditions

The environmental conditions at the lowering operation are not known, but a rough estimate of the wind and waves will be made. This is intended to represent a storm occurring during the lowering operation, and the resulting environmental loads on the SCS will be studied. First the wind will be studied using wind data from weather stations nearby and the wave height and period will be estimated using fetch limitied waves theory.

### 3.2.1 Wind conditions at lowering site

The wind condition in Sør-Trøndelag can be found from a number of weather stations. A wide variety of wind data from the early 50's until present date are available on [Eklima]. This is free information available on the web. The problem is to choose a weather station that experiences the same wind velocities and profiles as the site where the SCS would is to be lowered.

First the weather station at Voll in the city of Trondheim was chosen. It is located approximately 4 km from the fjord, but the wind measured here will depend strongly on the wind direction due to the shape of the landscape surrounding the weather station. The measured wind values must be transformed from onshore values to mid fjord values, but the relationship is not known.


Figure 15 - Weather station at Voll


Figure 16 - Weather station at Værnes

A much better weather station is one located at Værnes Airport in Nord Trøndelag which provides much more usable wind data. The station is located on the same line as the longest fetch in the fjord of Trondheim to the location of the planned operation, and due to the landing strip on the air port there are very few obstacles such as buildings or trees that could obstruct the wind flow when the wind comes along the longest fetch.

The weather stations provide a large amount of statistical data with a short list presented in Table 6.

| Main observations |
|---|
| **Average of wind velocity** |
| **Lowest wind velocity** |
| **Highest wind velocity** |
| **Average of highest average wind values** |

Table 6 - Weather station main obersvations

As a rough estimate of the strong wind the “highest wind velocity” was assumed to represent a continuously high wind. Wind gust are neglected. Measurements month by month for the last 60 years was chosen. (Chapter A.5). The wind is measured 10 [m] above ground and 12 [m] above sea level, so it is assumed that the wind velocity at this altitude does not change significantly from over sea to over land.

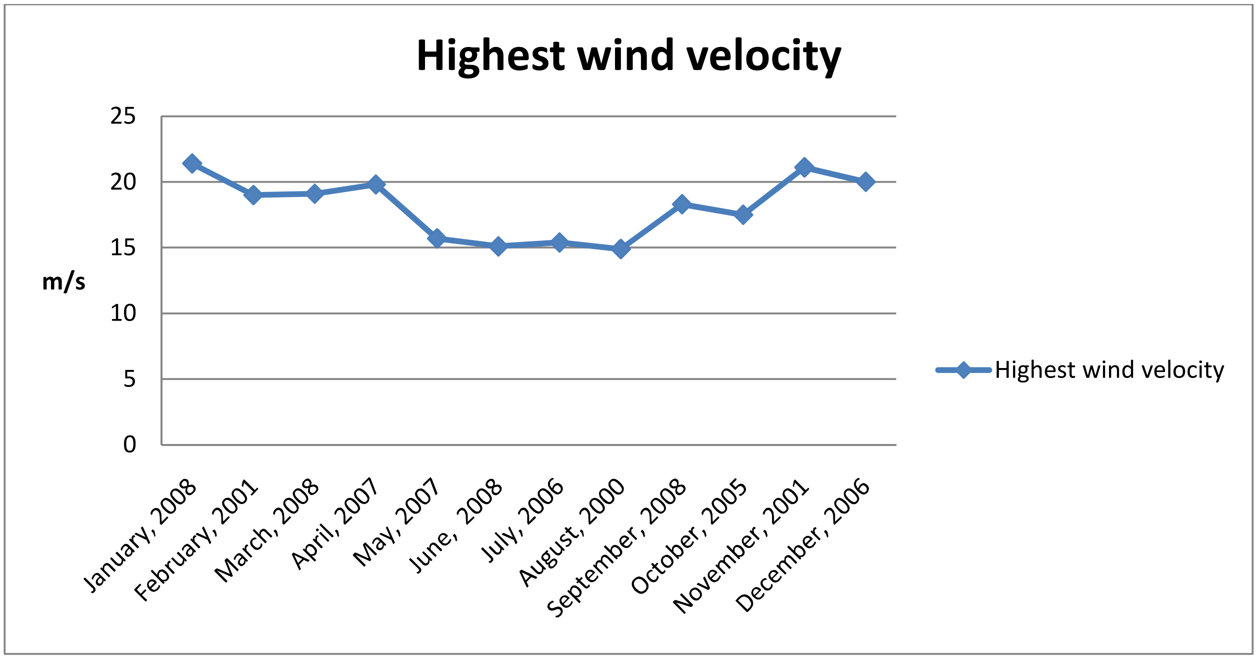


**Figure 17 - Plot of highest continuously wind month by month**

The highest wind velocity for each month independent of year is plotted in Figure 17. The figure clearly shows a trend where the highest wind velocity is lowest in the summer months May to August, and the operation is planned to be conducted in this time window. A maximum wind velocity of 16 $[{}^{m}/_{s}]$ is therefore assumed to be a rough estimate for high wind during bad weather in the summer. The actual direction of these winds has not been analyzed, but it is assumed that the high wind has the same direction as the maximum fetch line.

### 3.2.2 Wave conditions at lowering site

The waves inside the fjord of Trondheim will be pure wind generated waves with limited fetch, as no swell from the open sea will be able to reach the lowering operation site. The maximum fetch to this location is roughly measured to be 50 [km]. This fetch will be used to estimate the wave height.


**Figure 18 - Maximum fetch to the lowering operation site**

As a rough estimate of the wave height and wave period it is assumed that the waves can be described by the two parameters

1. Significant wave height $H_s$ - the mean wave height of the one third highest waves.
2. The wave period corresponding to the peak frequency of the spectrum $T_m$.

The two parameters are estimated using the empirical formulas found in [Carter 82] which discusses wind generated sea with limited fetch.

$$H_s = 0.0163X^{0.5}U \tag{3.1}$$
$$T_m = 0.566X^{0.3}U^{0.4} \tag{3.2}$$

where

| | |
|---|---|
| $X$ | Fetch in km |
| $U$ | Wind speed at 10 m above the sea surface in $m/s$ |

Estimating locally generated wind sea

| | | | | |
|---|---|---|---|---|
| U | ***16*** | m/s | **<= INPUT** | |
| X | ***50*** | km | **<= INPUT** | |
| 1.71*U^2 | 593.92 | | | <= limit fetch |
| type | **JONSWAP** | | <= OUTPUT | |
| | | | | |
| Hs | **1.84** | m | <= OUTPUT | |
| Tm_01 | **5.5** | s | <= OUTPUT | |

**Table 7 - Wind generated sea with limited fetch**

By assuming deep water waves, the wave length may be estimated from the period $T_m$.

| Wave data | Value | Dimension |
|---|---|---|
| **Significant wave height $H_s$** | 1.84 | $[m]$ |
| **The mean wave period $T_m$** | 5.5 | $[s]$ |
| **Wavelength $\lambda$** | 47.2 | $[m]$ |
| **Water depth at location C in Figure 2** | $200 \pm 20$ | $[m]$ |

**Table 8 - Estimated wave conditions at lowering site**

## 3.3 Simple model of lowering operation of the SCS through the sea surface

The lowering operation of the SCS is a complex operation, and to be able to simulate this operation using software, simplifications need to be made. The first simplification is to reduce the 6 degrees of freedom to the heel motion only. This heel motion of the barges is then represented by two dynamic one mass systems. The second simplification is to reduce the buoyancy force from the trapped air in the SAs to nonlinear vertical springs. The third simplification is to reduce the environmental loads to first order wave forces on the SAs.

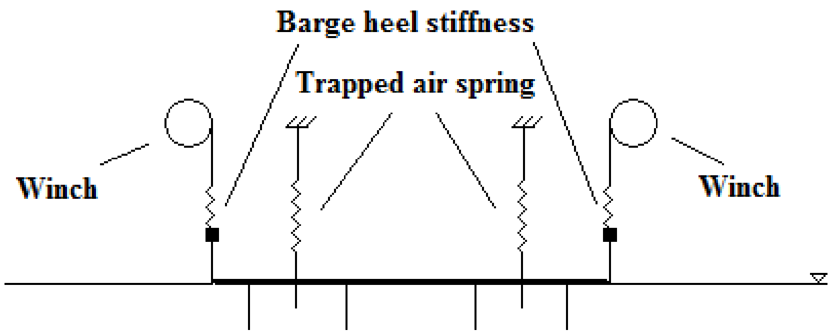


Figure 19 - Simple model of lowering operation of the SCS

### 3.3.1 Modeling the compressibility of air

The compressibility of air effect of the trapped air is crucial for the lowering operation of the SCS with respect to the buoyancy force. The first step in understanding the behavior of the trapped air is therefore to establish the buoyancy force and investigate how this change as the SAs is displaced up and down. A second step is to establish how the trapped air pressure changes if the water surface inside the SA is displaced up and down when keeping the SAs fixed.

It is assumed that the rate of which the trapped air is compressed and expanded can be separated into a high frequency and a low frequency compression and expansion. The high frequency compression and expansion is due to the first order wave motion, and the low frequency compression and expansion is due to the motion of the SCS which is assumed to be much slower than the wave period. The result from each analysis will be a set of linear force equations for the high frequency compression and expansion and a set of linear buoyancy force equations for the low frequency compression and expansion.

#### High and low frequency compression and expansion of trapped air

The motivation for trapping air inside the SAs is the resulting buoyancy force contribution. The pressure and volume of the trapped air is crucial with regards to the magnitude of the buoyancy force, and the amount of compression and expansion of the trapped air is therefore of great importance. The trapped air is assumed to follow the ideal gas law (Eq. 2.6). To fully understand the physics involved, first only one SA will be studied. The amount of trapped air needed to keep correct buoyancy must first be established. The dimensions of a SA are listed in (Chapter 3.1.1), where one SA has a height $12\ [m]$ and a radius $10\ [m]$. The internal water plane area is:

$$A_{SA} = \pi r_{SA}^2 = 314.16\ [m^2] \tag{3.3}$$

The weight load on one SA is the dry weight of the SCS divided by four, but the pre tension of the four wires from the two barges must also be subtracted from the weight. The dry weight of the SCS is $8000\ [tonne]$ and the pretension in one wire is set to $500\ [tonne]$. The steel volume of one SA is assumed to be neglectable in terms of buoyancy force. The weight load on one SA:

$$W_{SA} = \frac{W_{SCS,dry}}{4} - F_{preTension} = \frac{8000}{4} - 500\ [tonne] = 1500\ [tonne] \tag{3.4}$$

The initial over pressure inside the SA in order for the SA to carry the weight load must then be

$$P_{initial} = \frac{W_{SA}g}{A_{SA}} = \frac{1500 \cdot 10^3[kg] \cdot 9.81 \left[\frac{m}{s^2}\right]}{314.16[m^2]} = 46839[Pa] = 0.4622[P_{atm}] \tag{3.5}$$

This over pressure is equal to a hydro static water differential head:

$$H_{Dispwater} = \frac{P_{initial}}{\rho g} = \frac{46839[Pa]}{1025\left[\frac{kg}{m^3}\right] 9.81\left[\frac{m}{s^2}\right]} = 4.66\ [m] \tag{3.6}$$

So the differential head of water $H_{Dispwater}$ is the amount of water that must be displaced inside the SA in order for the SA to carry the weight load. The absolute pressure inside the SA is directly related to the hydrostatic pressure $H_{static}$ as illustrated in Figure 20.

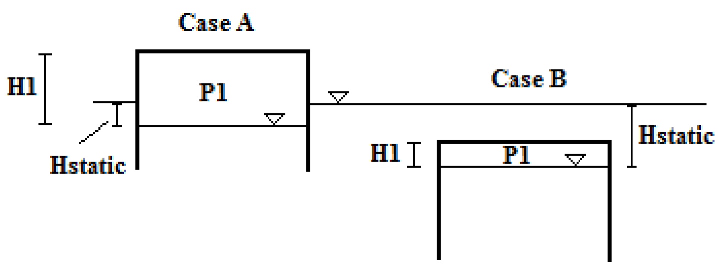


Figure 20 - Initial conditions

## High frequency compression and expansion

The high frequency compression and expansion is assumed to be directly linked to the first order wave motion and the vertical excitation of the water inside the SA. This compression and expansion will be in the same order as the first order wave period and is therefore assumed to be an adiabatic process with $n = \kappa = 1.4$.

The SA is assumed to be fixed because the high mass and moment of inertia of the SCS is assumed to give a very small acceleration over one wave period. The water plane area $A_{SA}$ inside a SA will be displaced up and downwards a known distance and the resulting absolute pressure will be calculated. The force acting on the water plane is then found by multiplying the over pressure by the water plane area. The water plane area is assumed to be constant.

For each initial depth selected, the buoyancy force is assumed to be equal to the weight $W_{SA}$ before the SA is displaced. The initial conditions is

$$P_1 \tag{3.7}$$

and

$$H_1 \tag{3.8}$$

The water plane surface is then displaced $H_{heave}$ where downwards is defined as positive. The new internal trapped air differential head will then be

$$H_2 = H_1 + H_{heave} \tag{3.9}$$

The pressure $P_2$ is found by the ideal gas law (Eq. 2.6).

$$P_2 = \left[\frac{H_1}{H_2}\right]^{\kappa} P_1 \tag{3.10}$$

where $\kappa = 1.4$

The force acting on the water surface plan:

$$F_{Watersurf} = \Delta P A_{SA} = (P_2 - P_1)A_{SA} \tag{3.11}$$

The force will be 0 when the displacement $H_{heave}$ is zero, negative the $H_{heave}$ is positive and positive when $H_{heave}$ is negative.

### Low frequency motion

The low frequency motion is linked to the motion of the SCS and more accurately the vertical and roll displacement of the SCS. This motion will be much slower than the first order wave period and is therefore assumed to be an isotherm process with $n = 1.0$.

The SCS will have a heave or roll motion, but only one SA is modeled so the SA is assumed to only have a vertical motion. The motion of the SA is assumed to have a much longer period than the first order wave motion and therefore the first order wave motion will be averaged out.

The behavior of the buoyancy force due to the trapped air changes as the SA becomes submerged, and two methods of calculating the buoyancy force contributions are shown. Case A where the SA is floating and case B where the SA is submerged.

For each initial depth selected, the buoyancy force is assumed to be equal to the weight $W_{SA}$ before the SA is displaced. The initial conditions is

$$P_1 \tag{3.12}$$

and

$$H_1 \tag{3.13}$$

The initial conditions are now established and the SA can be displaced a distance $H_{heave}$ in z-direction. The ideal gas law (Eq. 2.6) is used to find the new differential head $H_2$, but then a problem occurs. The new pressure $P_2$ and internal trapped air $H_2$ are both unknown, and they are both dependent on each other. So by assuming that the differential head $H_2$ is equal to $H_1$, the new pressure $P_2$ will be

$$P_2 = P_1 + \rho g H_{heave} \tag{3.14}$$

The new differential head $H_2$ is then found by using the ideal gas law.

$$H_2 = \left[\frac{P_1}{P_2}\right]^{\frac{1}{n}} H_1 \tag{3.15}$$

where $n = 1.0$

The pressure $P_2$ can now be estimated more accurately using the newly calculated $H_2$

$$P_2 = P_1 + \rho g (H_{Heave} + H_2 - H_1) \tag{3.16}$$

The process is continued until the solution converges.
The new buoyancy force from the trapped air due to the displacement $H_{Heave}$ will now be the over pressure multiplied by the internal surface area $A_{SA}$ for the case A - floating SA

$$F_{Buoyancy} = (P_2 - P_{atm}) A_{SA} \tag{3.17}$$

And the weight force due to the displaced water for case B – submerged SA

$$F_{Buoyancy} = \rho g H_2 A_{SA} \tag{3.18}$$

### Initial positions

To illustrate the change in trapped air stiffness as the SA is lowered down, 9 different initial positions are chosen. The buoyancy is assumed to be in balance with the weight $W_{SA}$ at the initial position and the SA is displaced up and down 2 [m]. The different initial positions are listed in Table 9 and shown in Figure 21. It is assumed that these 9 positions illustrate the important changing behavior of the trapped air. An important notice must be taken, the water level is assumed to be at $z = 0$ and changing water elevation in form of waves is not taken into account. This is strictly linear theory, and therefore the initial position at 12 [m] is split into two cases dependent on the direction of the heave motion since the SA will instantly go from floating to submerged as the SA is submerged more than 12 $[m]$.

| Name | Depth of SA | Dimension |
|---|---|---|
| $\boldsymbol{H_6}$ | 6 | $[m]$ |
| $\boldsymbol{H_8}$ | 8 | $[m]$ |
| $\boldsymbol{H_{10}}$ | 10 | $[m]$ |
| $\boldsymbol{H_{12}^{z<H_{SA}}}$ | 12, only displacing shallower | $[m]$ |
| $\boldsymbol{H_{12}^{z>H_{SA}}}$ | 12, only displacing deeper | $[m]$ |
| $\boldsymbol{H_{14}}$ | 14 | $[m]$ |
| $\boldsymbol{H_{16}}$ | 16 | $[m]$ |
| $\boldsymbol{H_{18}}$ | 18 | $[m]$ |
| $\boldsymbol{H_{20}}$ | 20 | $[m]$ |
| $\boldsymbol{H_{22}}$ | 22 | $[m]$ |

Table 9 - SA depths

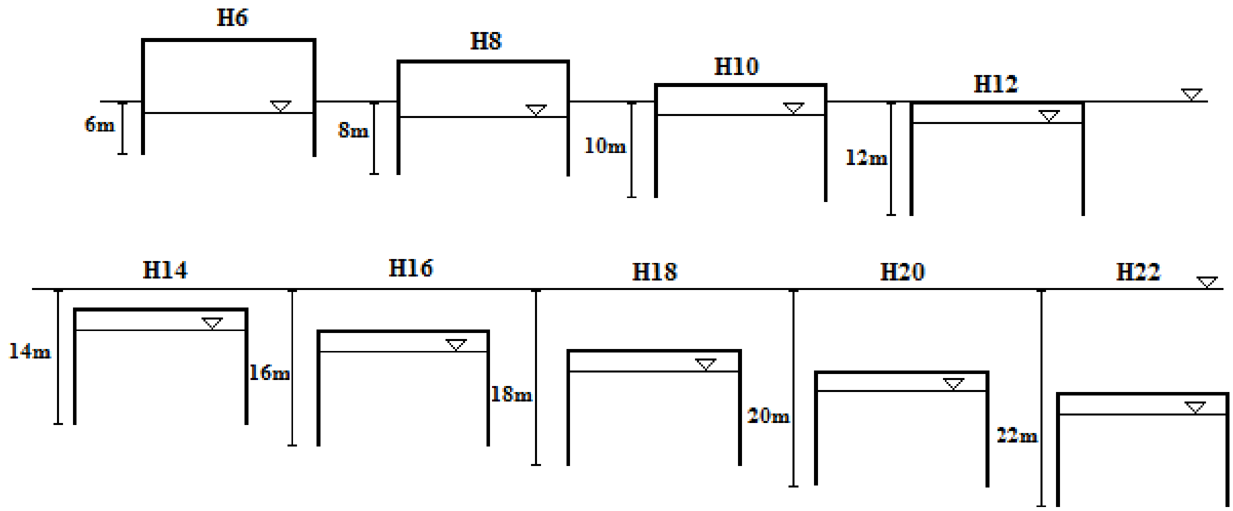

Figure 21 - SA depths

### Result high frequency compression and expansion

$$F_{High\ frq\ force} = aZ + b \tag{3.19}$$

Where $Z$ is the vertical displacement of the SA and $a$ and $b$ are defined in Table 10.

| Name | Initial depth *[m]* | Gradient, a *[MN/m]* | Constant, b *[MN]* |
|---|---|---|---|
| $H_6$ | 6 | -6.1149 | 0 |
| $H_8$ | 8 | -7.5279 | 0 |
| $H_{10}$ | 10 | -9.7904 | 0 |
| $H_{12}$ | 12 | -13.998 | 0 |
| $H_{14}$ | 14 | -15.898 | 0 |
| $H_{16}$ | 16 | -17.798 | 0 |
| $H_{18}$ | 18 | -19.698 | 0 |
| $H_{20}$ | 20 | -21.598 | 0 |
| $H_{22}$ | 22 | -23.498 | 0 |

Table 10 - Gradient and constant for high frequency linear spring

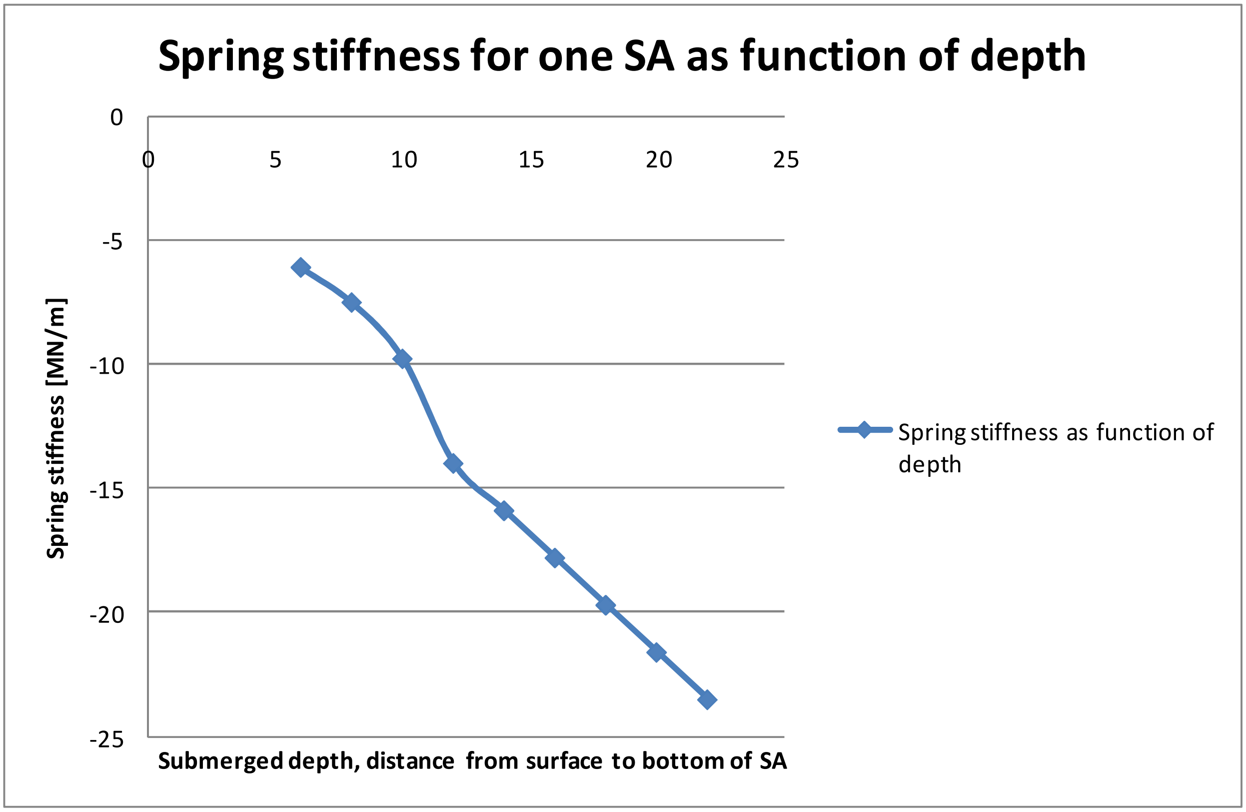


Figure 22- Plot of gradient for high frequency linear spring

Figure 22 shows that as the SA is lowered deeper and deeper, the trapped air volume becomes stiffer and stiffer.

### Result low frequency compression and expansion

$$F_{Buoyancy} = cZ + d \qquad (3.20)$$

Where $Z$ is the vertical displacement of the SA and $c$ and $d$ are defined in Table 11.

| Name | Initial depth *[m]* | Gradient, c *[MN/m]* | Constant, d *[MN]* |
|---|---|---|---|
| $\boldsymbol{H_6}$ | 6 | 1,5703 | 14,715 |
| $\boldsymbol{H_8}$ | 8 | 1,9078 | 14,715 |
| $\boldsymbol{H_{10}}$ | 10 | 2,1572 | 14,715 |
| $\boldsymbol{H_{12}^{z<H_{SA}}}$ | 12, only displacing shallower | 2,3915 | 14,715 |
| $\boldsymbol{H_{12}^{z>H_{SA}}}$ | 12, only displacing deeper | -0,75285 | 14,715 |
| $\boldsymbol{H_{14}}$ | 14 | -0,68784 | 14,715 |
| $\boldsymbol{H_{16}}$ | 16 | -0,62903 | 14,715 |
| $\boldsymbol{H_{18}}$ | 18 | -0,57949 | 14,715 |
| $\boldsymbol{H_{20}}$ | 20 | -0,53718 | 14,715 |
| $\boldsymbol{H_{22}}$ | 22 | -0,50063 | 14,715 |

Table 11 - Gradient and constant for low frequency linear spring

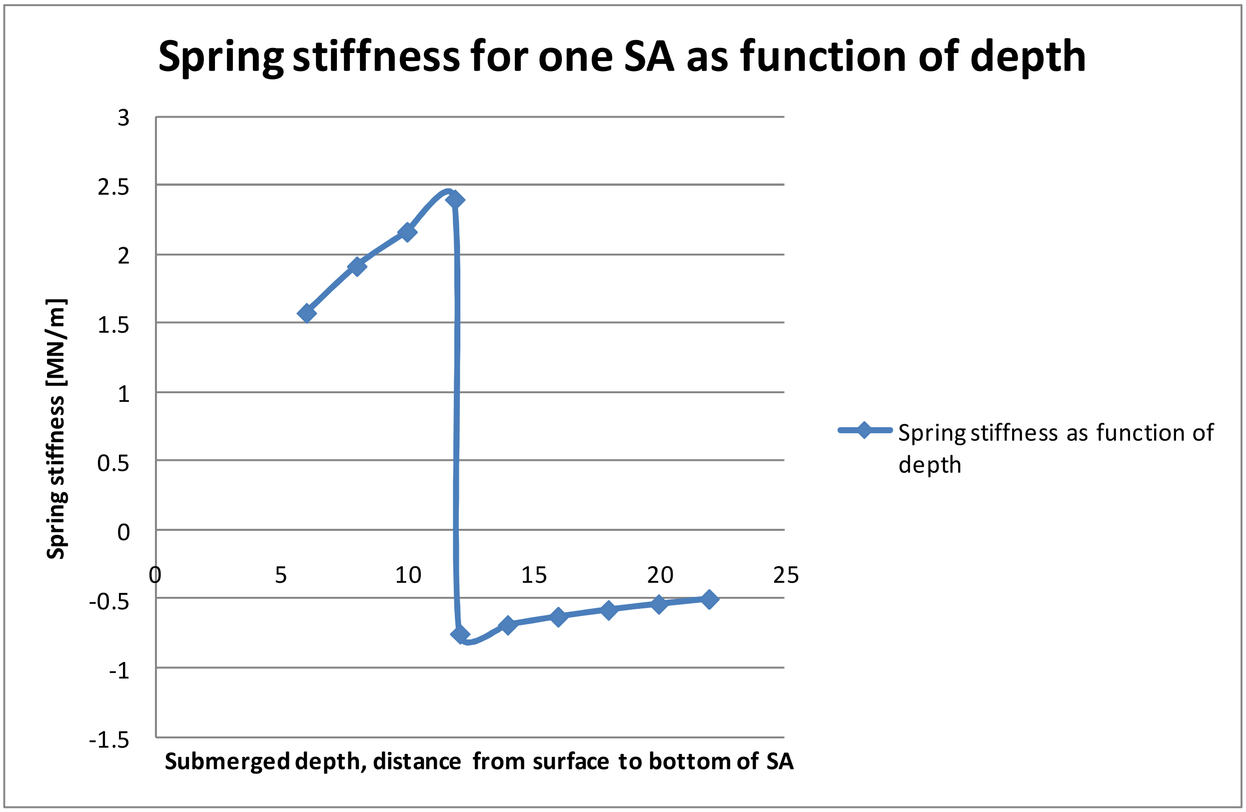


Figure 23 - Plot of gradient for low frequency linear spring

Figure 23 shows the in trapped air stiffness and how it changes dramatically when the SA becomes submerged.

### 3.3.2 Estimating hydrodynamic forces

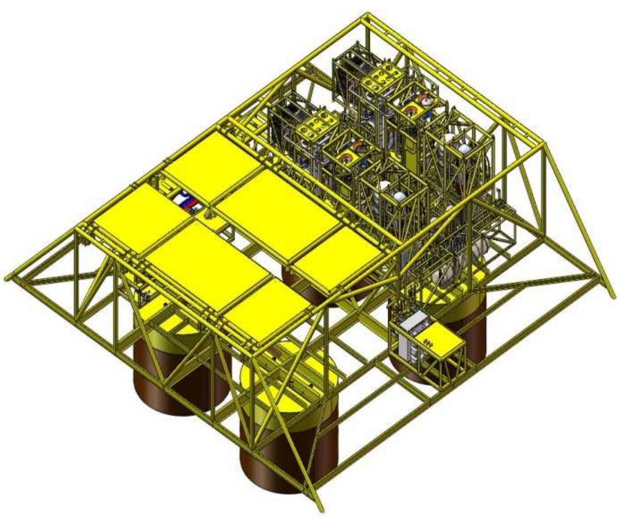

Figure 24 - Illustration of the SCS

The SCS module consists of a very complex geometry structure along with four compressor trains and four SAs. The hydrodynamic forces are due to the complexity not easy to predict, but a rough estimate of the added mass of the SCS will be estimated. The damping is neglected in order to keep the model simple.

### Estimation of added mass of a SA

The magnitude of the added mass of the SAs in both vertical and horizontal direction are large due to the SAs size. To roughly estimate the magnitude of this added mass, [DNV 08] and estimates are used.

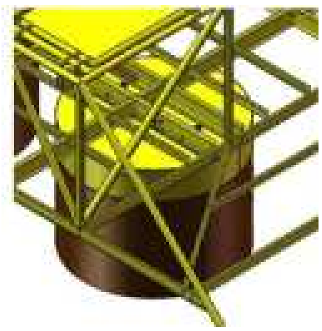

Figure 25 - Illustration of a SA

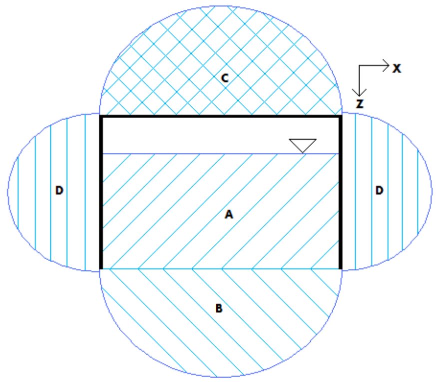


Figure 26 - Rough estimate of the distribution of added mass of a SA

The added mass of the SA can be separated into masses dependent on the direction of motion.
As the SA is oscillated in the z - direction, the added mass area A and B will be oscillated along with the surface of the trapped air. However, the acceleration of added mass A and B does not need to be in phase with the acceleration of the SA. The excitation forces and the compressibility of air effect of the trapped air determines how large the phase difference may be.

The added mass C gives a pressure distribution on the top of the SA which is in phase with the acceleration of the SA in z-direction. However, the top of the SA is attached to the subsea structure and so the added mass C will be included in the added mass calculation of the SCS structure.

The added mass A is the internal volume of the SA subtracted of the trapped air volume. The volume will change as the trapped air is compressed or expanded but for small displacements the volume is close to constant. The trapped air volume will also change dependent on what level the SCS floats.

$$A_{33,A} = \rho(H_{SA} - H_1)\pi R_{SA}^2 \tag{3.21}$$

The added mass B is assumed to be a half sphere with the radius same as the SA.

$$A_{33,B} = \frac{2}{3}\rho\pi R_{SA}^3 \tag{3.22}$$

The added mass D is assumed to equal the added mass of a flat plate which is oscillated in non restricted deep water where the flat plate is the projection of the SA in the same direction. The acceleration of added mass D will always be in phase with the acceleration of the SA. The general formula for calculating added mass in x- and y-direction along with the needed coefficients according to [DNV 08, pp. 96-97] is then

$$A_{ii} = \rho C_A V_R \tag{3.23}$$

which then becomes

$$A_{11,D} = A_{22,D} = \rho C_A V_R \tag{3.24}$$

| Added mass coefficent | $C_A$ | $V_R$ |
|---|---|---|
| $\boldsymbol{A_{11,D} = A_{22,D}}$ | $= 0.62$ | $\pi R_{SA}^2 H_{SA}$ |

Table 12 - Added mass coefficients from [DNV 08 pp. 96-97]

### Results

| Added mass | One SA | Four SAs | Dimension |
|---|---|---|---|
| **A** | 2864 | 11456 | [$tonne$] |
| **B** | 2147 | 8587 | [$tonne$] |
| **A+B** | 5011 | 20044 | [$tonne$] |
| **D** | 2396 | 9583 | [$tonne$] |

Table 13 - Added mass estimation for the SAs

### Estimation of the added mass of the SCS structure

To find the added mass to the SCS without the SA attached is a very difficult task without making large simplifications. First simplification is that only the center box marked with red in Figure 27 contributes to added mass. Secondly, this box is assumed to have a fill ratio of 50% which means that half the box is trapped water and the rest is equipment and structural components. Third the loss of surface area on the low side of the box due to the presence of the SA is accounted for by including a loss of area coefficient $C_{corr,SA}$ which is estimated.

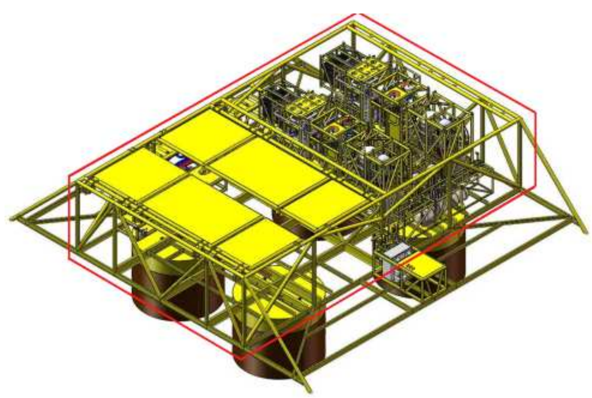

Figure 27 - SCS simplification

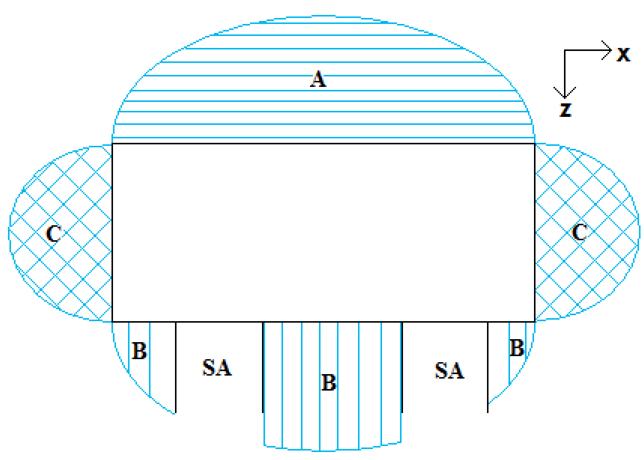


Figure 28 - Rough estimate of added mass distribution of the SCS

| Dimension of red box | Value | Dimension |
|---|---|---|
| $\boldsymbol{L_{box}}$ | $30 + 2 \cdot 10 = 50$ | $[m]$ |
| $\boldsymbol{B_{box}}$ | $80$ | $[m]$ |
| $\boldsymbol{H_{box}}$ | $27 - 12 = 15$ | $[m]$ |

**Table 14 - Dimensions of simplified SCS**

The added mass C is assumed to equal the added mass of a flat plate which is oscillated in non restricted deep water where the flat plate is the projection of the SCS in the same direction. The general equation (Eq. 3.23) is then used. However, the water closed within the box must also be included and is estimated to be

$$A_{trapped} = \rho L_{SCS} B_{SCS} H_{SCS} C_{fill} \tag{3.25}$$

where $C_{fill}$ is assumed to be 50%.
The added mass in x- and y-direction is then

$$A_{11,total} = A_{trapped} + A_{11} \tag{3.26}$$

$$A_{22,total} = A_{trapped} + A_{22} \tag{3.27}$$

The added mass in z-direction consists of A and B illustrated in Figure 28. A and B is assumed to equal the added mass of a flat plate which is oscillated in non restricted deep water where the flat plate is the projection of the SCS in the same direction, however B is corrected due to the presence of the SAs.

$$A_{33} = \rho C_A V_R C_{corr,SA} \tag{3.28}$$

where $C_{corr,SA}$ tries to correct for the surface area lost due to the presence of the SA.The correction is estimated by subtracting the top area of all four SAs from the total surface area on the top and bottom combined, and divided by the total surface area.

$$C_{corr,SA} = \frac{(2 \cdot L_{box} \cdot B_{box} - 4 \cdot A_{SA})}{2 \cdot L_{box} \cdot B_{box}} \tag{3.29}$$

The total added mass in z- direction with acceleration in phase with the acceleration of the SCS or box is then

$$A_{33,total} = A_{trapped} + A_{33} \tag{3.30}$$

| Added mass coefficent | $C_A$ | $V_R$ |
|---|---|---|
| $\boldsymbol{A_{11}}$ | $\approx 0.900$ | $\frac{\pi}{4} H_{SCS}^2 B_{SCS}$ |
| $\boldsymbol{A_{22}}$ | $= 0.757$ | $\frac{\pi}{4} H_{SCS}^2 L_{SCS}$ |
| $\boldsymbol{A_{33}}$ | $= 0.704$ | $\frac{\pi}{4} L_{SCS}^2 B_{SCS}$ |

**Table 15 - Added mass coefficients from [DNV 08, pp. 96-97]**

**Results**

| Added mass | Value | Unit |
|---|---|---|
| $A_{trapped}$ | 30750 | $[tonne]$ |
| $A_{11}$ | 13041 | $[tonne]$ |
| $A_{11,total}$ | 43792 | $[tonne]$ |
| $A_{22}$ | 6856 | $[tonne]$ |
| $A_{22,total}$ | 37606 | $[tonne]$ |
| $A_{33}$ | 95213 | $[tonne]$ |
| $A_{33,total}$ | 125963 | $[tonne]$ |

Table 16 - Added mass estimation for the SCS

### 3.3.3 Modeling barge heel stiffness

The heel motion of the barges is an important part of the lowering operation of the SCS. As the SCS is lowered down and the buoyancy force of the trapped air change, the barges must change the heel angle to account for this change in buoyancy force. Effectively the weight of the SCS is transferred between the buoyancy force of the trapped air and the wires to the barges.

The dynamic heeling motion of a barge is assumed to be described as

$$(I_{55} + A_{55})\ddot{\theta} + B_{55}\dot{\theta} + C_{55}\theta = F_{wire}\frac{B_B}{2}\theta \tag{3.31}$$

where

| | |
|---|---|
| $I_{55}$ | Moment of inertia in roll |
| $A_{55}$ | Added mass in roll |
| $B_{55}$ | Linear damping in roll |
| $C_{55}$ | Linear stiffness in roll |
| $F_{wire}$ | Downwards force in wire |
| $B_B$ | Total width of barge |
| $\theta, \dot{\theta}, \ddot{\theta}$ | Heel angle, velocity and acceleration |

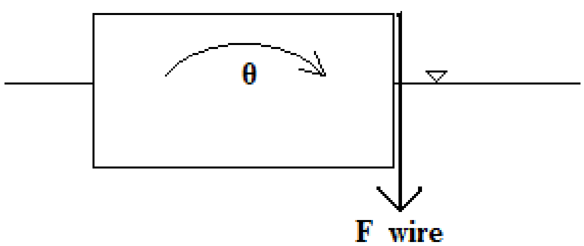


Figure 29 - Heel motion of barge

Damping $B_{55}$ and added mass $A_{55}$ is unknown and is for simplicity assumed to be zero. Moment of inertia $I_{55}$ was supplied by Aker Solutions for a standard North Sea barge. Stiffness $C_{55}$ is calculated using linear stability theory. Excitation moment $F_{wire}\frac{B_B}{2}\theta$ is due to the weight load from the SCS. (Eq. 3.31) can now be simplified to

$$I_{55}\ddot{\theta} + C_{55}\theta = F_{wire}\frac{B_B}{2}\theta \tag{3.32}$$

The angle $\theta$ can be related to the vertical displacement $Z_{SCS}$ of the wire connection point of the SCS. Small angles and displacement are assumed.

$$Z_{SCS} = \frac{B_B}{2}\theta \rightarrow \theta = \frac{2}{B_B}Z_{SCS} \tag{3.33}$$

Inserting (Eq. 3.33) into (Eq. 3.32)

$$I_{55}\frac{2}{B_B}\ddot{Z}_{SCS} + C_{55}\frac{2}{B_B}Z_{SCS} = F_{wire} \tag{3.34}$$

The mass term will then be

$$\widehat{M} = I_{55}\frac{2}{B_B} \tag{3.35}$$

The linear stiffness is found using linear stability theory. The derivation is shown in (Chapter A.1)

$$GM_B = \frac{2B_B^2 - 3H_B^2}{12H_B} \tag{3.36}$$

$$\nabla_B \rho g GM_B \theta_B = F_{wire}\frac{B_B}{2} \tag{3.37}$$

The stiffness term $\hat{C}$ is then when inserting (Eq. 3.36) and (Eq. 3.37)

$$\hat{C} = C_{55}\frac{2}{B_B} = \frac{F_{wire}}{Z_{SCS}} = \frac{4\nabla\rho g GM_B}{B_B^2} \tag{3.38}$$

The mass $\widehat{M}$ will be suspended in the spring, so the spring must be stiffened to account for this.

$$\overline{C} = \hat{C}Z_{SCS} + \widehat{M}g \tag{3.39}$$

**Result**

| Name | Value | Unit |
|---|---|---|
| $\hat{C}$ | 7778.4 | $[kN/m]$ |
| $\widehat{M}$ | 53284 | $[tonne]$ |
| $\widehat{M}g$ | 522716 | $[kN]$ |

Table 17 - The one mass dynamic system input representing heel motion of barge

# 4 Modeling in SIMO

## 4.1 Modeling wave forces on SAs

To model the SAs on the SCS requires an analysis of the wave forces the SAs experiences. Only first order wave forces are considered and SIMO's slender elements will be used due their simplicity and versatility through the user specified input. However, the first modeling problem in SIMO occurs when the SAs are to be modeled with the correct hydrodynamic properties. Normally, a SA would be modeled by one slender element. However, slender elements use Morison's equation, which finds wave forces on small volume submerged structures. The problem is the large diameter of a SA, as the requirement for validity of Morison's equation is $(D/\lambda) < 0.2$, but for the SA the ratio is $(2R_{SA}/\lambda) = 20/47.2 \approx 0.42$ if the environmental conditions found in (chapter 3.2) is used. The significant wave height is $H_S = 1.84\ [m]$ and the corresponding wave period is $T_m = 5.5\ [s]$.

### 4.1.1 First order wave forces in surge and sway

If slender elements is to be used to model the SAs, the resulting first order wave forces needs to be compared with other methods. The result from SIMO will therefore be compared with the results from a model created in Genie and analyzed in HydroD and with hand calculations. To establish if the number of slender elements affects the results, two SIMO models where the SAs are modeled with one or six slender elements are tested. All the models are assumed to be fixed because the response motion of the SCS is not known and so by setting the models to be fixed makes it easier to compare them.

| Name of model | One SA model | Four SAs models | Theory | Fixed/floating |
|---|---|---|---|---|
| **SIMO – simple model** | 1 Slender Element | 4 Slender Elements | Morrison's equation | Fixed |
| **SIMO – complex model** | 6 Slender Elements | 24 Slender Elements | Morrison's equation | Fixed |
| **Hydro D - model** | 1 solid cylinder created in Genie | Resulting load from 1 Solid cylinder extrapolated to four cylinders | Radiation-diffraction theory employing a panel model | Fixed |
| **Hand calculation** | 1 solid cylinder | Resulting load from 1 Solid cylinder extrapolated to four cylinders | Linear wave potential | Fixed |

Table 18 - List of the four SA models

To compare if the submersion of the SA affects the results between the different methods, four different depths were chosen.

| Name | Depth | Dimension |
|---|---|---|
| $\boldsymbol{H_6}$ | 6 | $[m]$ |
| $\boldsymbol{H_8}$ | 8 | $[m]$ |
| $\boldsymbol{H_{10}}$ | 10 | $[m]$ |
| $\boldsymbol{H_{12}}$ | 12 | $[m]$ |

Table 19 - Chosen depths of SA

### 4.1.2 SIMO- simple model

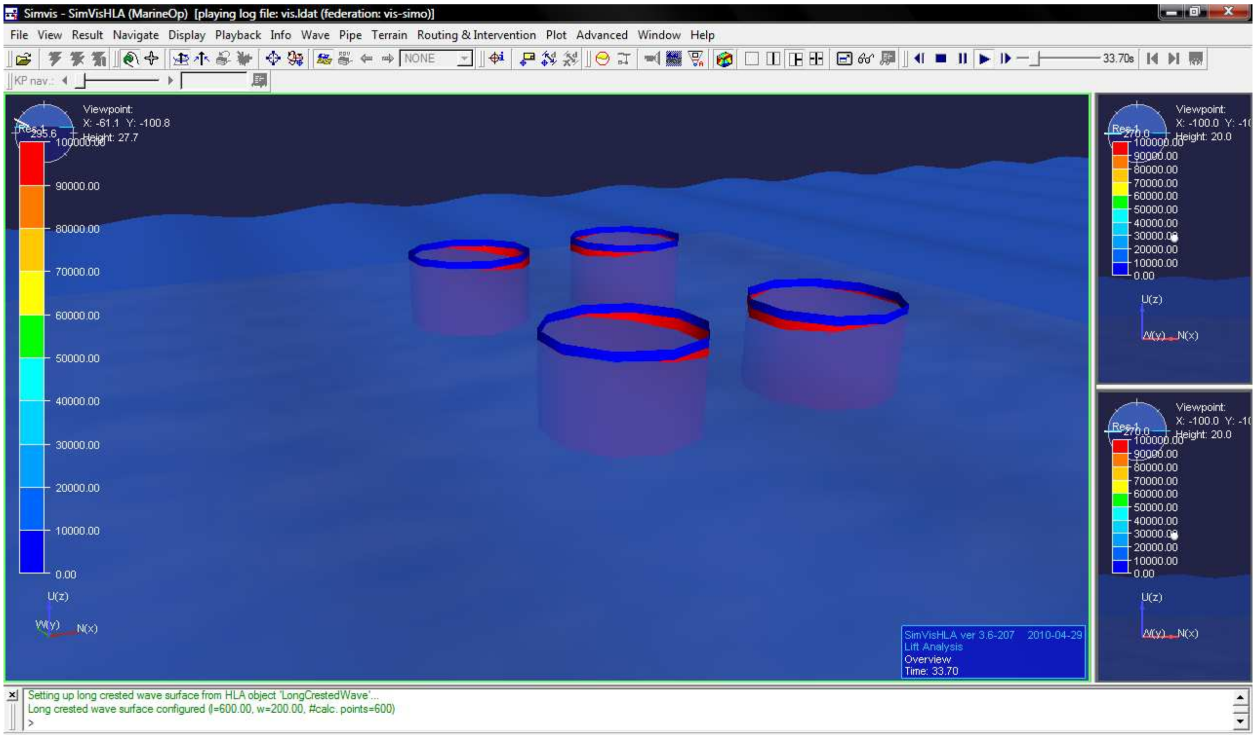


Figure 30 - SIMO simple model

#### 4.1.2.1 Slender element

Each SA is modeled by one slender element with the same disk area as the SA defined through SPEVOL.
$SPEVOL = \pi * r^2 = \pi * 10^2 [m^2] = 314.16 [m^2]$

The weight of the element is of no importance as long as the model is set to fixed.
$\mathrm{DSTMAS} = 0\ [\mathrm{Tonne/m}]$

The force is integrated to actual wave elevation
$IFOADD = 1$

The gravity and buoyancy force is of no importance
$IVOL = 1$

Wave particle velocity and acceleration is included
$IWDHF = 2$

The number of strips is set to 10
$NSTRIP = 10$

All drag forces are assumed to be zero.
$C2X = C2Y = C2Z = C1X = C1Y = C1Z = 0$

The added mass per unit length is found from chapter XX. All these units are given in the local coordinate system.

$AMX = 0$

$$AMY = AMZ = \frac{Total\ added\ mass\ in\ global\ x - or\ y - direction}{Height\ of\ SA}$$

$$AMY = AMZ = \frac{2864 + 2396}{12} \frac{[tonne]}{[m]} = 438.33 \frac{[tonne]}{[m]}$$

```
'=============================================================
 DISTRIBUTED ELEMENT FORCES
'=============================================================
'
' Descriptive text, 2 lines
  SA represented by one
  slender element
'============================================================
'SLENDER ELEMENT
'============================================================
'SPEVOL DSTMAS IFOADD IVOL IWDHF NSTRIP
'XEL1 YEL1 ZEL1 XEL2 YEL2 ZEL2 XREF YREF ZREF
'C2X C2Y C2Z C1X C1Y CIZ AMX AMY AMZ
'
'Suction Anchor #1
SLENDER ELEMENT
314.16     0.    1     1     2     10
-15.  -25.  0.    -15.  -25.  -12.  -15.  -36.  -12.
0.    0.    0.    0.    0.    0.    0.    438.33     438.33
```

#### 4.1.2.2 Environmental data specification

The wave load is defined as a regular wave with wave height $H_S$ and wave period $T_m$.

```
'*************************************************************
ENVIRONMENT DATA SPECIFICATION
'*************************************************************
'
'Descriptive test, 3 lines
Regular wave
Waveheight 1.84 m
Wave period 5.5 second
'--------------------------
 REGUlar WAVE SPECification
'--------------------------
'   1 input line
'   CHREWA - Regular wave condition identificator
 CHREWA
'NREGWA
 1
'
'WAVAMP WAVPER PHASE  DIR
0.92  5.50  0.0   0.0
'---------------------------------------------------------
'*************************************** end of Environmental
```

### 4.1.3 SIMO – complex model

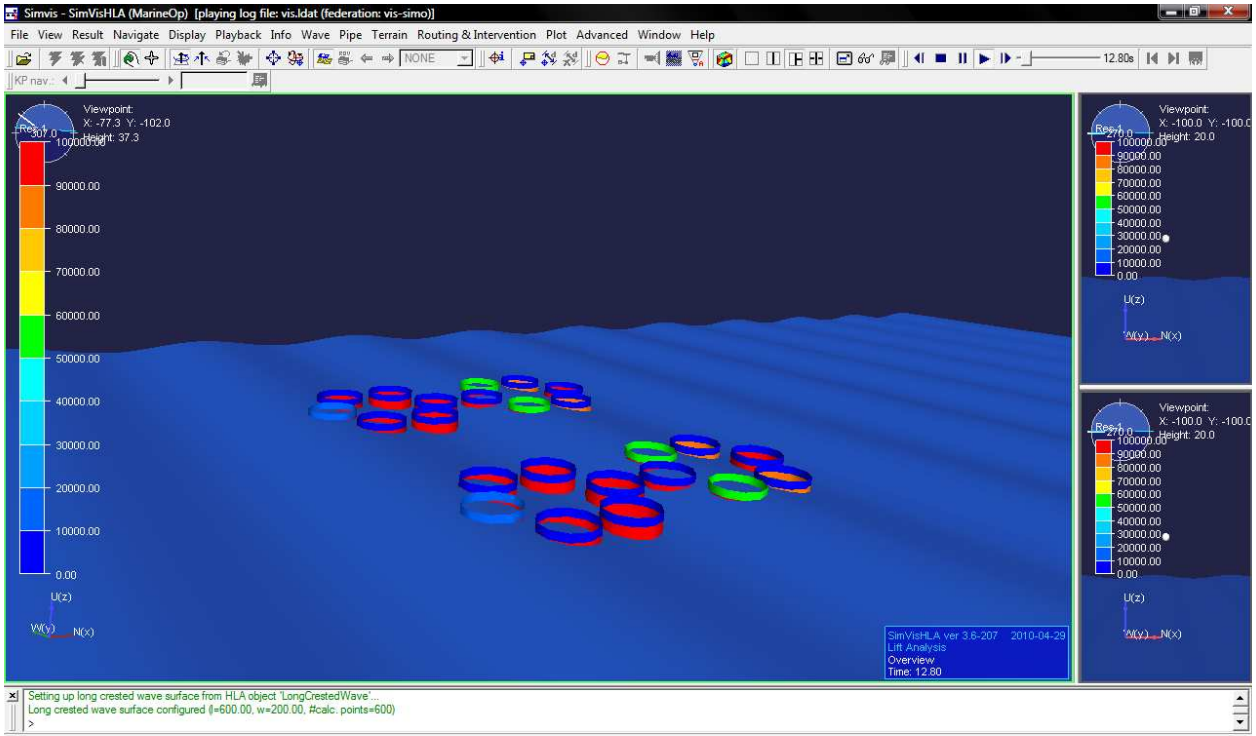


Figure 31 - SIMO complex model

Each SA is now modeled by six slender elements with the same total disk area as the SA defined through SPEVOL. The load for each SA will now be distributed on 6 Slender Elements instead of 1. For this case the wave elevation is almost uniform over one small disk, which indicates that the result from the complex model should be more able to capture the varying wave loads over the diameter of the SA than the simple model. The only change in input from the simple model is the $SPEVOL$ and the added mass $AMY$ and $AMZ$.

$$SPEVOL = \frac{\pi * r^2}{6} = \frac{\pi * 10^2}{6}[m^2] = 52.36[m^2]$$

$$AMY = AMZ = \frac{\dfrac{Total\ added\ mass\ in\ global\ x - or\ y - direction}{Height\ of\ SA}}{6}$$

$$AMY = AMZ = \frac{\dfrac{2864 + 2396}{12}\dfrac{[tonne]}{[m]}}{6} = 73.06\frac{[tonne]}{[m]}$$

```
'=============================================================

 DISTRIBUTED ELEMENT FORCES
'=============================================================
'
' Descriptive text, 2 lines
  SA represented by one
  slender element
'============================================================
'SLENDER ELEMENT
'============================================================
'SPEVOL DSTMAS IFOADD IVOL IWDHF NSTRIP
'XEL1 YEL1 ZEL1 XEL2 YEL2 ZEL2 XREF YREF ZREF
'C2X C2Y C2Z C1X C1Y CIZ AMX AMY AMZ
'
'Suction Anchor #1
'
SLENDER ELEMENT
52.36   0.      1       1       2       10
-25.0   -25.0   0.0     -25.0   -25.0   -12.0   -25.0   -24.0   -12.0
0.      0.      0.      0.      0.      0.      0.      73.06   73.06
 SLENDER ELEMENT
52.36   0.      1       1       2       10
 -20.0  -33.7 0.0 -20.0 -33.7 -12.0 -20.0 -34.0 -12.0
 0.     0.      0.      0.      0.      0.      0.      73.06   73.06
 SLENDER ELEMENT
52.36   0.      1       1       2       10
 -10.0  -33.7 0.0 -10.0 -33.7 -12.0 -10.0 -33.0 -12.0
0.      0.      0.      0.      0.      0.      0.      73.06   73.06
 SLENDER ELEMENT
52.36   0.      1       1       2       10
 -5.0  -25.0 0.0 -5.0 -25.0 -12.0 -5.0 -24.0 -12.0
0.      0.      0.      0.      0.      0.      0.      73.06   73.06
 SLENDER ELEMENT
52.36   0.      1       1       2       10
 -10.0  -16.3 0.0 -10.0 -16.3 -12.0 -10.0 -16.0 -12.0
0.      0.      0.      0.      0.      0.      0.      73.06   73.06
 SLENDER ELEMENT
52.36   0.      1       1       2       10
 -20.0  -16.3 0.0 -20.0 -16.3 -12.0 -20.0 -16.0 -12.0
0.      0.      0.      0.      0.      0.      0.      73.06   73.06
```

### 4.1.4 HydroD-model

A 3-D panel model of a cylinder with the radius and height of a SA is created in GeniE. The cylinder has closed top and bottom.

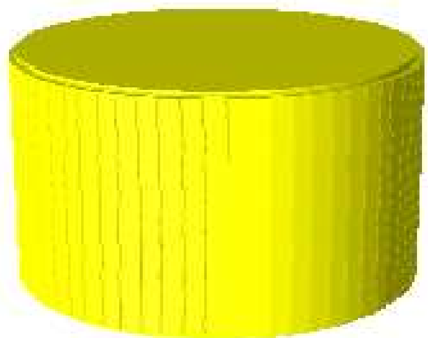

Figure 32 - GeniE model

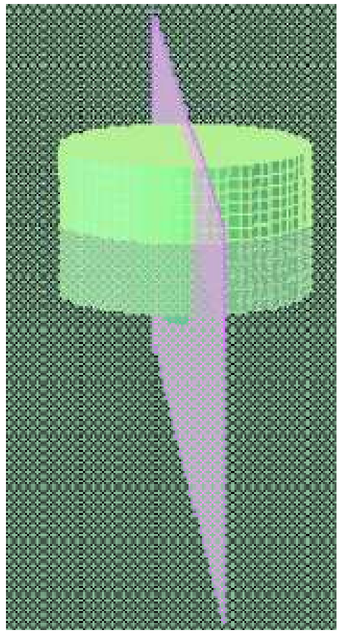

Figure 33 - HydroD model

The model was exported to HydroD, and the linear 3-D radiation-diffraction theory employing panel model was used to find the first order wave force. The regular wave period $T_m = 5.5\ s$ and the four depths listen in Table 19 were used. The cylinder was set to fixed and the result from the analysis are the first order wave force on a single SA for each depth. To account for all the four SAs, the load delay from first SA to back SA was calculated using the known wave speed and the known distance from center of front SA to back SA. The result is multiplied by 2 to account for the other two SAs.

$$F_{waveload,amp} = 1.521 A_{load} \tag{4.1}$$

The derivation of the equation (Eq. 4.1) is shown in (Chapter A.2).
The command files to Genie and HydroD is located in (Chapter A.7).

### 4.1.5 Analytical model

When the cylinder is as large as one SA relative to wavelength, Morrison's equation becomes invalid as pointed out in the beginning of this chapter. However, to find the first order wave load on such a structure, one may use MacCamy and Fuchs theory [Marin 07 pp. 2.44-2.45]. This method is analytical and deals with the spreading of a sinus wave from a circular cylinder located at the sea bottom and reaches up through the sea surface. As long as linear potential theory is used, the method is accurate for all diameters of the cylinder.

If the cylinder is great ($\lambda/D\ \ is\ small$) the method gives the total load because the drag force neglectable, and for smaller cylinders ($\lambda/D\ \ is\ great$) the method gives the same result as the mass-term in Morrison's equation. To show that the drag force becomes very small, one can assume that the wave motion around the cylinder consists of one regular wave and an infinite sum of reflected ring shaped waves that spread from the cylinder.

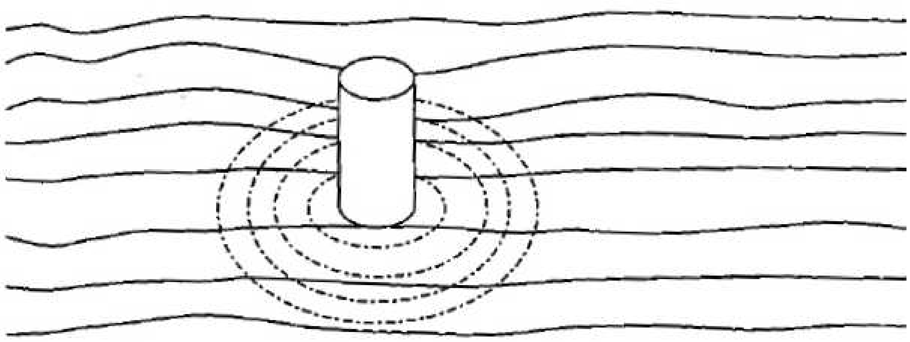

**Figur 2.34 Innkomne og reflekterte bølger fra sylinder**

Figure 34 - Wave pattern [Marin 07, figure 2.34]

By demanding that no fluid shall penetrate the cylinder surface, one can find the velocity potential for the ring shaped waves (diffraction potential $\phi_D$). The potential for regular incoming waves ($\phi_I$), together with $\phi_D$, gives the total potential $\phi_T = \phi_I + \phi_D$. When the total potential is known, one can calculate the pressure distribution around the cylinder and so the horizontal load per unit length, $dF$.

$$dF = \frac{2\rho g H}{k}\frac{\cosh\big(k(z+h)\big)}{\cosh(kh)}A(ka)\cos(\omega t - \epsilon) \tag{4.2}$$

Where $A(ka)$ is a load amplitude factor and $\epsilon$ is the phase delay from wave to load.

The values for $A(ka)$ and $\epsilon$ is found from table 4 in [Marin 07 pp. 2.46-2.48]

$$ka = \frac{\omega^2}{g}r = 1.61 \tag{4.3}$$

which gives the values $A(ka) = 1.5496$ and $\epsilon = 8.86$

The total load for one cylinder can then be found by simply integrating the load $dF$over the height of the cylinder. The total load on all the SAs are included by

$$F_{waveload} = 1.521A_{load} \tag{4.4}$$

The derivation of the equation (Eq. 4.4) is shown in (Chapter A.2).

### 4.1.6 Results

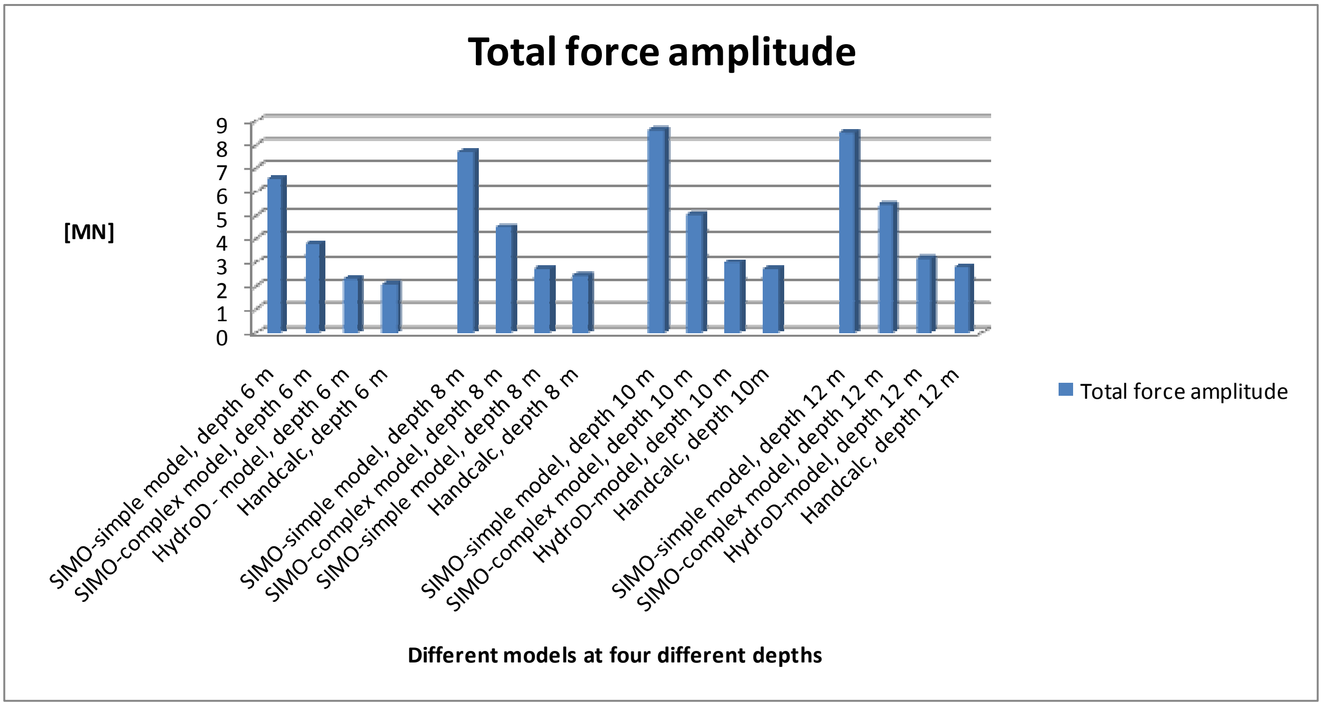


**Figure 35 - First order wave force amplitude**

The Figure 35 shows clearly that increasing the number of slender elements from one to six elements per SA reduces the total first order wave load on all four SAs. The results from the HydroD-model and hand calculations are close to each other and closest to the SA represented with six slender elements. The SAs is therefore assumed to be best represented by six slender elements each, still the result will be conservative compared to the HydroD and hand calculation. The depth does not seem to affect the difference between the different results. The reason for that the complex model gives a better result that the simple model may the assumption that the wave conditions are constant over the diameter of the slender elements is pore for the simple model.

## 4.2 Procedure – SIMO

When the necessary input values had been found, they were inserted into the system description file. SIMO could then execute a time domain simulation based on the system description file and calculate the environmental induced loads and motions on the specified bodies and wires. The operation was visualized in SimVis.

The following chapter explains the input to the system description file and what parameters SIMO uses to numerically calculate the time domain simulation. The system description files and visualization files is located in (Chapter A.8).

### 4.2.1 Lowering operation of the SCS

The goal of the SIMO simulation of the operation is to find the heel angle of the barges, the force in the wires and the buoyancy forces from the trapped air as the SCS is lowered down. The initial depth of the SAs is set to 11 [m], meaning that the SAs are 1 [m] for being fully submerged. The SCS is then lowered slowly down by releasing 2 [m] of wire from the winches on the two barges. It is assumed that at the initial depth of the SAs of 11 [m], 6000 [$tonne$] of the 8000 [$tonne$] dry weight of the SCS is carried by

the trapped air inside the SAs. The last $2000$ [$tonne$] is carried through the four wires. No air is added or released as the SCS is lowered down and as discussed in (Chapter 3.3.1), the air is assumed to follow an isotherm process. The end result is presented in form of graphs and discussed.
The SIMO model is a simplified model of the full scale lowering operation of the SCS. Figure 36 shows the final model, and although the model does not visually resemble the SCS and barges, the important physical properties are included. Three bodies are defined; one body for each of the barges and one body for the SCS.

### 4.2.2 Barges

The main motion of the barges that is of interest is the heel motion. As a simplified model, the other five degrees of freedom is neglected and the barge can be represented by a dynamic one mass system.

#### Body type 3

The barges are simulated as body types 3, which has three degrees of freedom. The body is free to move in $x-, y-$and $z - direction$, but is not allowed to rotate. This reduces the amount of input required and is the simplest model when a dynamic one mass system is modeled. To model the barges as body type 3 requires the following data groups:

- Body location data
- Body mass data
- Position system data
- Body components

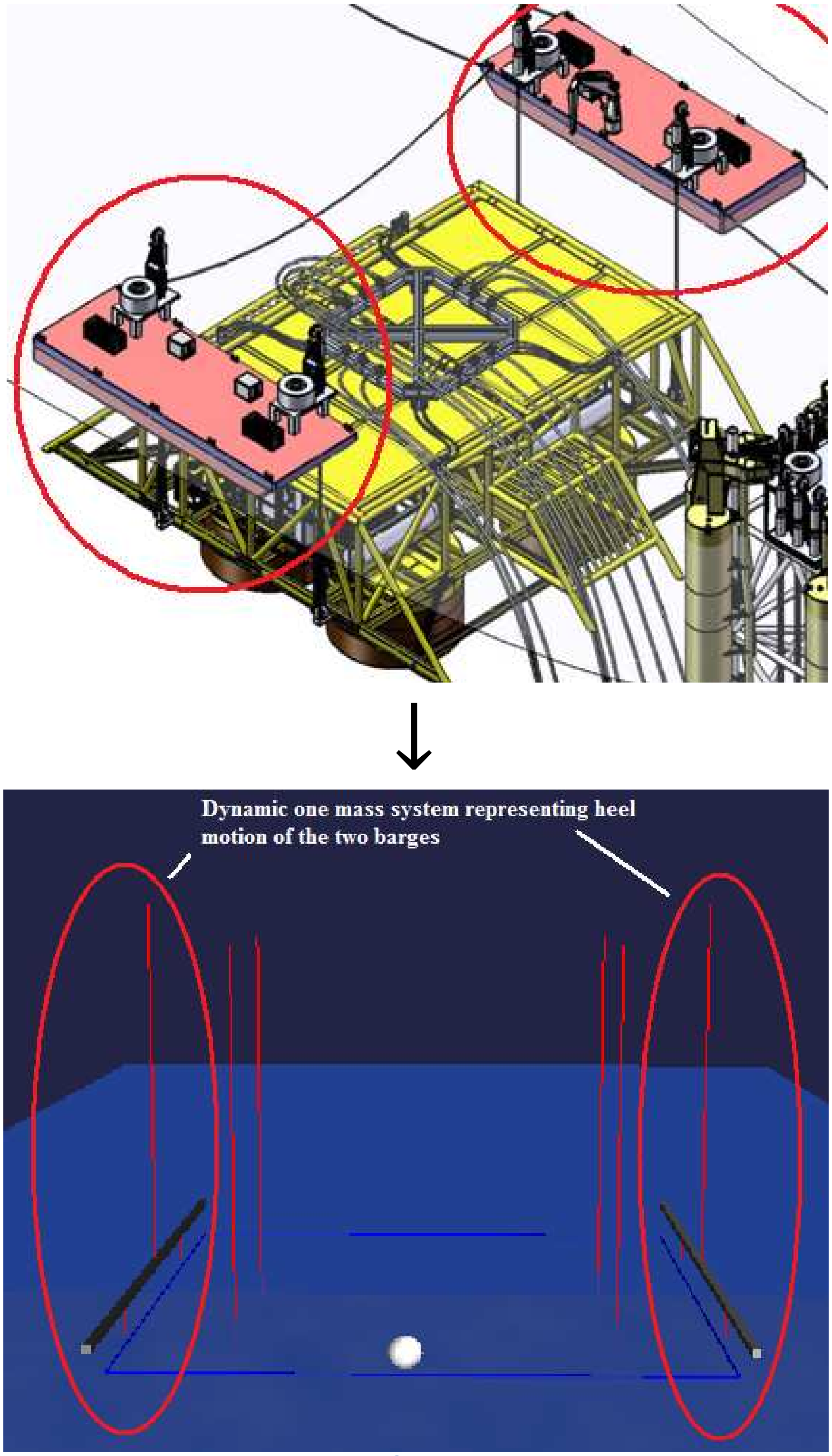

Figure 36 – Comparison between the full scale barges and SIMO barges models

For each barge the long red line represents the heel stiffness $\overline{C}$ (Eq. 3.39), while the long black element represents the mass $\widehat{M}$ (Eq. 3.35). The two short wires represent the wires connecting the strand jack to the SCS.

### Body location data

The two bodies are positioned alongside the SCS as illustrated in Figure 36.

| Body name | Global X-coordinate | Global Y-coordinate | Global Z-coordinate | Dimension |
|---|---|---|---|---|
| **Barge1** | 0 | 38 | 5 | $[m]$ |
| **Barge2** | 0 | -38 | 5 | $[m]$ |

Table 20 - Barge bodies global coordinates

### Body mass data

Both bodies are given the mass $\widehat{M}$ (Eq. 3.35) which represents the moment of inertia $I_{55}$ of the barge multiplied with the arm from center of barge to the winches. Because a body type 3 cannot rotate, moment of inertia is set to zero.

```
rm        rixx      riyx      riyy      rizx      rizy      rizz
53284.    0.00      0.00      0.00      0.00      0.00      0.00
```

### Position system data

The hydrostatic heel stiffness of a barge is modeled by a fixed force elongation spring attached between the body and a fixed global point. If the body should move in x- and y-direction, a short spring would give considerable forces in the same direction which is not wanted. The spring length is therefore initially set to 50 [m] to avoid this. The spring carries the weight $\widehat{M}g$ when it is elongated 50 [m].

The force of the spring is found using (Eq. 3.39).

```
‘DIST  FORCE     DAMP       (Resulting heel angle of barge [deg])
 47.6  504054.4  10.        (-10.0)
 50.   522722.6  10.        (0.0)
 52.4  541390.8  10.        (10.0)
```

SIMO assumes a linear relationship between the forces as the spring is compressed or expanded, and extrapolates or interpolates if the displacement is between or outside the given data.

However, output from SIMO gives the force in the connection points of the spring and the resulting heel angles must then be back calculated from these results. A clever trick is to add a second very weak spring in parallel where the force for a given displacement is the actual heel angle in degrees. By plotting these results, the heel angle of the barge as a function of time is directly found. Since the spring is so week, it will not affect the result.

```
'DIST  FORCE     DAMP       (Resulting heel angle of barge [deg])
 47.6  -10.      10.        (-10.0)
 50.   0         10.        (0.0)
 52.4  10.       10.        (10.0)
```

### Body components

Two coupling points was assigned to each body, each with a fixed winch. These represent the strand jack system onboard the barges.

| Name Barge1 / Barge2 | Local X-coordinate | Local Y-coordinate | Local Z-coordinate | Unit |
|---|---|---|---|---|
| COPO_1 / COPO_3 | 22 | 0 | 0 | $[m]$ |
| COPO_2 / COPO_4 | -22 | 0 | 0 | $[m]$ |

**Table 21 - Coordinates of winches**

All four winches are assumed to release 2 [m] of wire simultaneously over a time of 360 seconds which corresponds to the suggested lowering speed $V_{Winch} = 20\,[m/h] = 0.00556\,[m/s]$.

```
'tstart    tstop      runvel
 120.      480.       0.00556
```

### 4.2.3 SCS

The SCS is modeled as a large body where the buoyancy force from the trapped air in the SAs is of interest as it is lowered down. The upper structure of the SCS along with the compressor trains are not modeled as only a small part of this structure will become submerged and it is assumed that the buoyancy contribution from this part is small compared to buoyancy from the trapped air.

**Body type 1**

The SCS is defined as a body type 1, with six degrees of freedom. To define the SCS as body type 2 would not work, because body type 2 requires a pre calculated linear response for a given load. When body type 1 is selected, SIMO calculates the response for a given load. To model the SCS as body type 1 requires the following data groups:

- Body location data
- Body mass data
- Distributed element forces
- Position system data

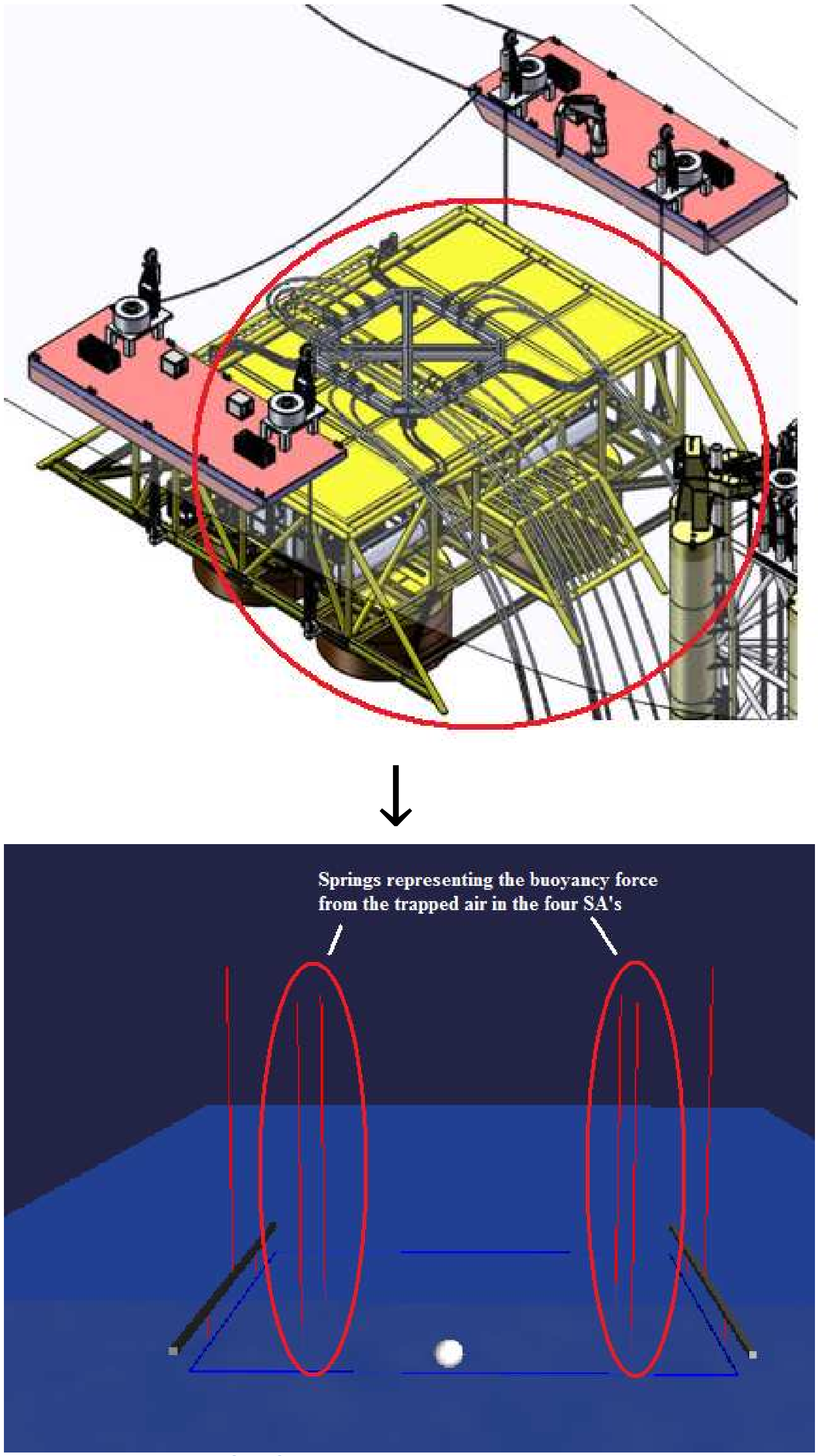


**Figure 37 - Comparison of the full scale SCS to the SIMO SCS model**

For the SCS the four red lines represent the buoyancy force from the trapped air in the four SAs.

### Body location data

The body is positioned in the center of the global coordinate system.

| Body name | Global X-coordinate | Global Y-coordinate | Global Z-coordinate | Dimension |
|---|---|---|---|---|
| **SCS** | 0 | 0 | 0 | *[m]* |

Table 22 - SCS body global coordinates

### Body mass data

The dry weight of the SCS is 8000 [tonne]. The body has the possibility to rotate, however the rotation of the body is very small as long as all four winches releases wire simultaneously, so the size of the moment of inertia needs only to be larger than zero to avoid numerical problems.

```
'rm        rixx       riyx       riyy       rizx       rizy       rizz
8000.      1000.      1000.      1000.      1000.      1000.      1000.
```

### Distributed element forces

The lower frame where the SAs are connected to the SCS is modeled with four slender elements. These are only for visualization purposes and are modeled to not give any force contribution.

The SIMO model of the SAs was found to give satisfying first order wave forces when each SA was modeled by 6 slender elements evenly spaced as explained in (Chapter 4.1). To avoid unwanted buoyancy contributions, the specific volume is set to zero and the added mass per meter is adjusted to include the loss of specific volume as discussed in (Chapter 2.4.2).

### Position system data

The buoyancy forces from the trapped air inside the SAs changes with depth and is modeled by four fixed force elongation springs. These are attached at the approximate center of the internal water surface inside a SA and a fixed global point above. If the body should move in x- and y-direction, a short spring would give considerable forces in the same direction which is not wanted. The spring length is therefore initially set to 50 [m] to avoid this. When the spring is elongated 50 [m], each spring carries 1500 [tone] of weight. The initial condition is set to a depth of 11 [m] marked with a black dot in the graph. No air is added or released and the buoyancy force is calculated using (Chapter A.4) which displace the SA 1 [m] up and 3 [m] down.

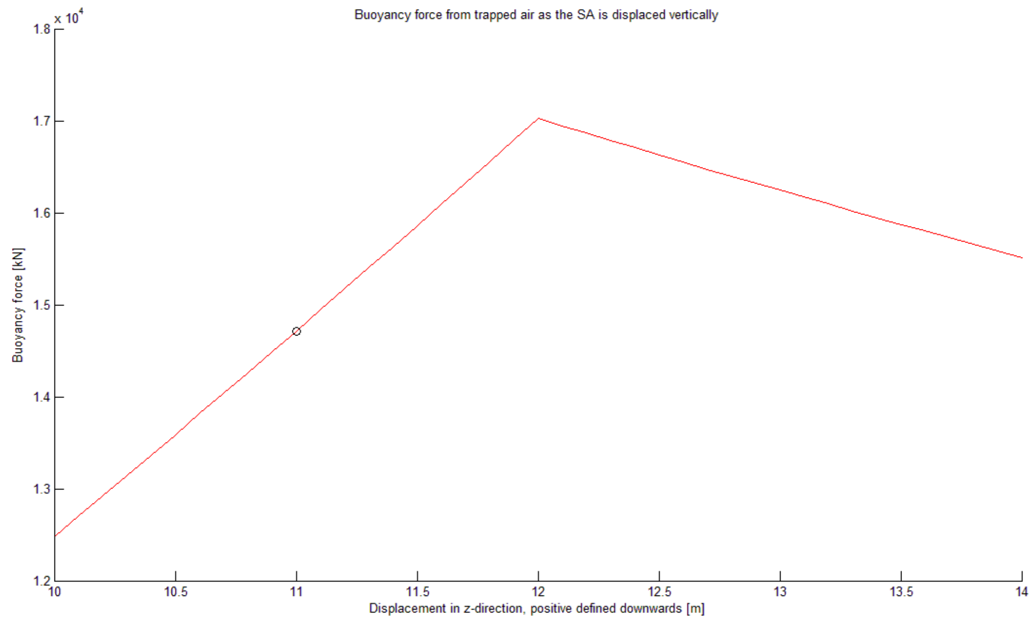

Figure 38 - Buoyancy force from one SA with depth of 11 m as initial position

```
DIST  FORCE       DAMP
49.   12439.9     30.
50.   14715       10.
51.   16990.1     10.
52.   16240.      10.
53.   15510.      30.
```

### 4.2.4 Running SIMO

A time domain analysis of the lowering operation of the SCS was made using SIMO modules STAMOD, DYNMOD and OUTMOD. Batch files for each of the modules were created and can be found in (Chapter A.8).

The SIMO model is highly specialized for the lowering operation of the SCS, and is valid only for a short vertical displacement of 4 [m] due to the trapped air inside the SAs. The most important results will be the tension in the wires, the reason is that the wire tensions along with how much wire is released are the only direct control the operators have over the motion of the SCS. As the SAs becomes submerged, more and more of the weight of the SCS will be transferred from the buoyancy of the trapped air to the barges.

**STAMOD**

Using the pre-generated batch file, STA.MAC, the system description file was read simultaneously defining the bodies and the couplings between them. Initial positions for all the bodies and body components are established. Static equilibrium was calculated for the entire system, and the initial wire force is updated along with the initial position of the SCS and the heel angle of the two barges. The result is described in ini.sam file which is read by DYNMOD.

| Initial conditions – Barge 1 and 2 | Value | Dimension |
|---|---|---|
| **Heel angle** | 2.8 | $[Deg]$ |
| **Wire load in one wire** | 262.8 | $[tonne]$ |

**Table 23 – Updated initial conditions for barges after equilibrium calculation**

| Initial conditions – SCS | Value | Dimension |
|---|---|---|
| **Vertical position of top of SAs** | 0.7 | $[m]$ |
| **Buoyancy load from one SA** | 1730.1 | $[tonne]$ |

**Table 24 – Updated initial conditions for SCS after equilibrium calculation**

**DYNMOD**

Using the pre-generated batch file, DYN.MAC, and the result from STAMOD, ini.sam, DYNMOD can perform a time domain simulation. The simulation and storage parameters are chosen so SIMO will not encounter numerical problems. For each oscillation of a body, SIMO requires that enough points are calculated so the motion can be described without jumps. This means that the time step must be sufficient small enough to cover the highest eigenfrequency of the whole system. The time step was set to $\delta t = 1\ [s]$ and the number of subdivision for each step was set to 100. The length of the time simulation was set to $600\ [s]$ and the Runge kutta integration method applying average acceleration over one time step suggested by SIMO was used. A visualization file, vis.ldat, was created and a copy is located in A.8.

**OUTMOD**

This module was used to extract the results from the time domain simulation. Wire force, heel angle of barge and buoyancy force were saved as ASCII-files and a copy is located in (Chapter A.8). The result was analyzed by MatLab.

### 4.2.5 Limitations

The motion of the barges was simplified to only the heel motion which was represented by a dynamic one mass system. This is a very simplified model, and it does not account for many important effects. No wave or wind loads on the barges are included, so this simplified barge model will give poor results when environmental conditions are applied.

Only the first order wave load on the SAs of the SCS is modeled. For more accurate environmental loads on the model of the SCS, higher order waves and wind loads should be included.

The modeling of the trapped air buoyancy force by the use of springs should be valid, but one must assume how this spring will behave. It may therefore take some trial and error if a specific result is desired since the springs are dependent on how the SCS behaves.

# 5 Results

## 5.1 SIMO simulation

The two SIMO simulations presented are both simulation of the same lowering operation of the SCS through the sea surface. The difference is that the first simulation, Case 1 – still water, is done without any waves, and the second simulation, Case 2 – worst weather condition, includes regular waves with heading in the x – direction in the SCS coordinate system defined in Figure 14. The wave height and period used is estimated in (Chapter 3.2).

The results from the two simulations show how the heel angle of one of the barges, wire loads and buoyancy loads changes as 2 [m] of wire is released from the winches. The top of the SAs are initially 0.7 [m] above the water surface and the SCS is in an equilibrium position. As the SCS is lowered down, no air is added or released. The result from each 6 [min] long simulation is presented in form of three graphs.

1. First graph shows the barge heel angle and one wire load, plotted versus time
2. Second graph shows the buoyancy load from one SA and one wire load, plotted versus time.
3. Third graph shows the total buoyancy load from all four SAs and the total wire load from all four wire loads, plotted versus time.

### 5.1.1 Case 1- Still water

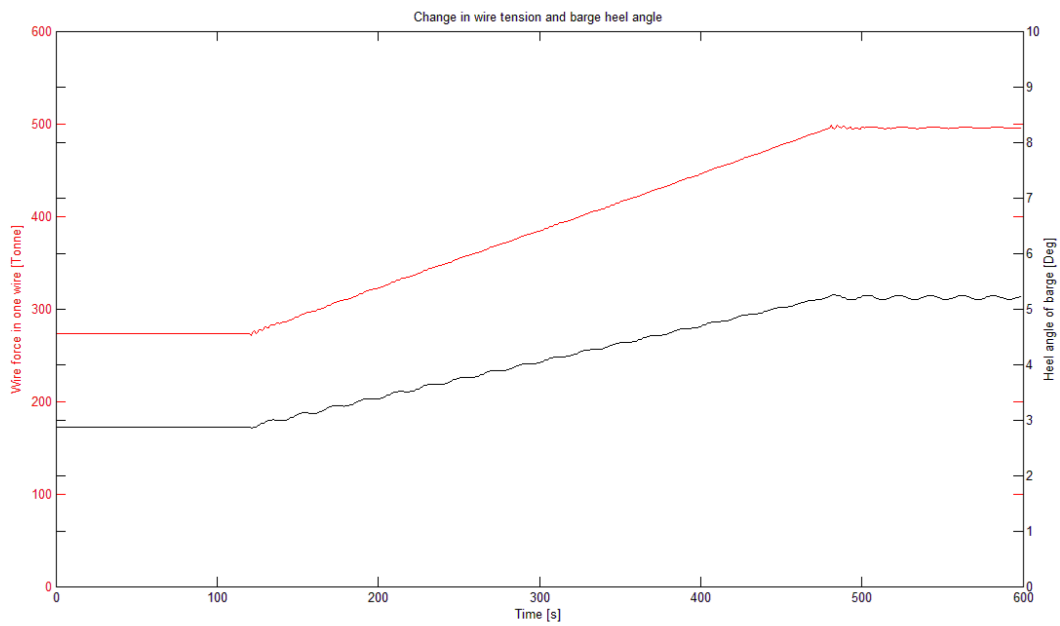


Figure 39 - Heel angle of one barge and the wire load in one wire

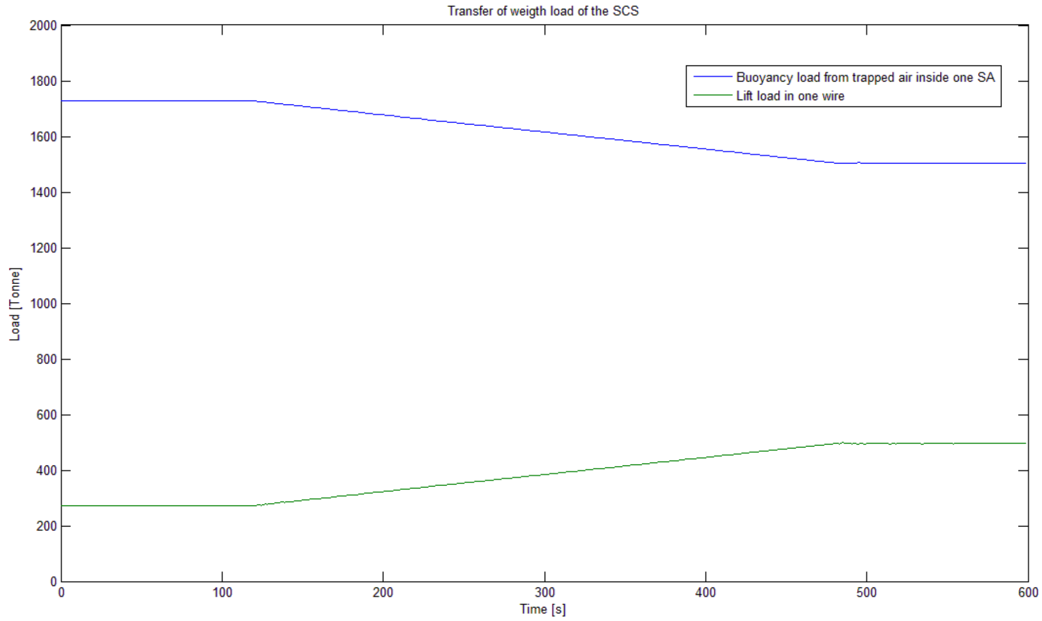


Figure 40 - load in one wire and buoyancy load from one SA

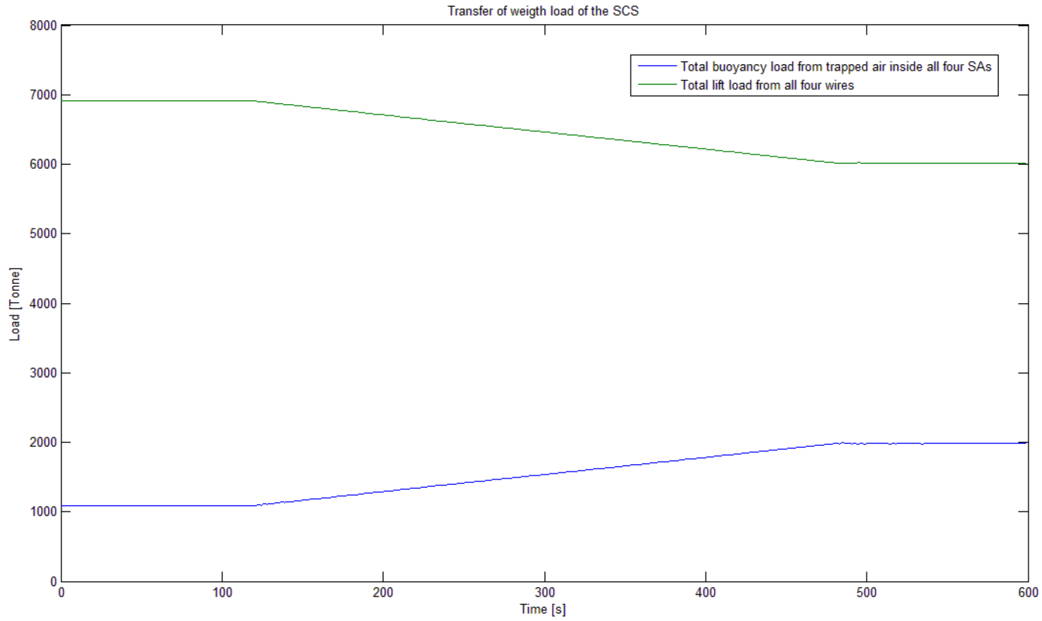


Figure 41 – Total wire load and total buoyancy load from the trapped air

### 5.1.2 Case 2 – Worst weather condition

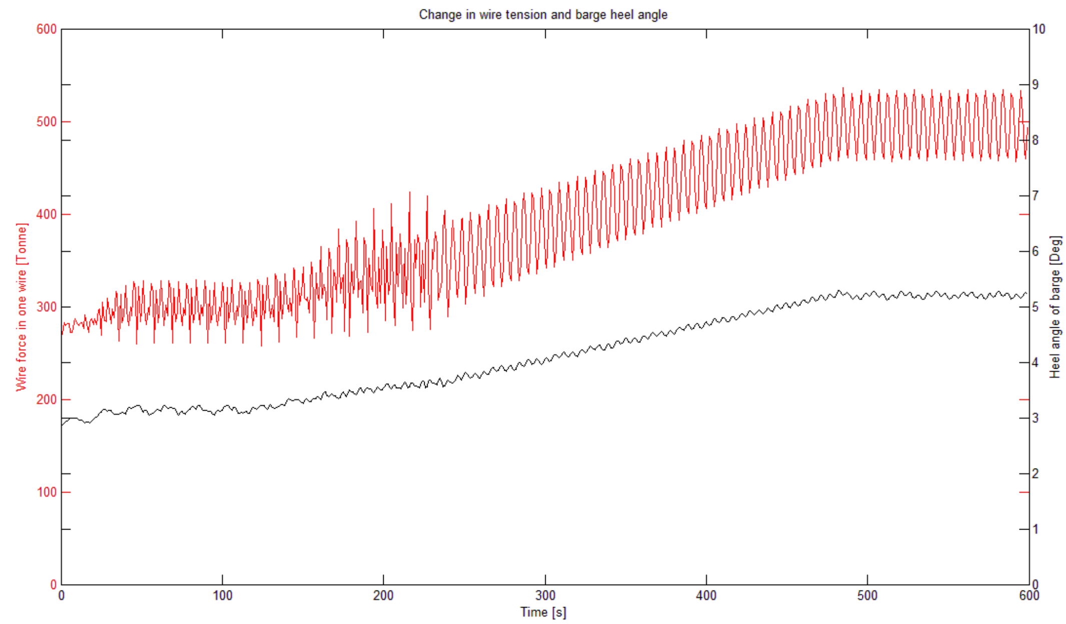


**Figure 42- Heel angle of one barge and the load in one wire**

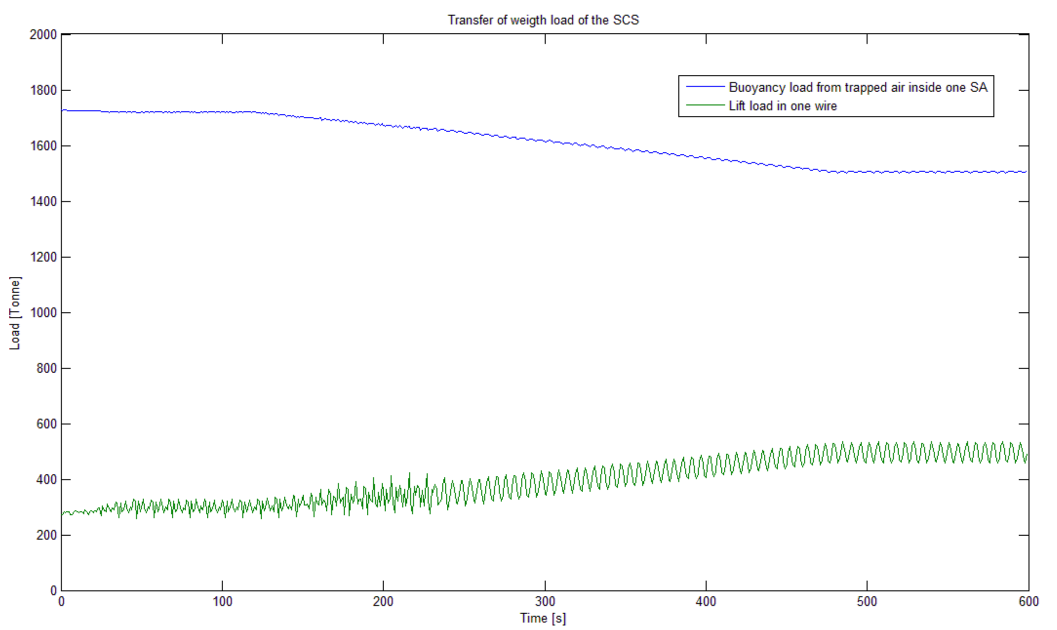


**Figure 43 Wire load in one wire and buoyancy load from one SA**

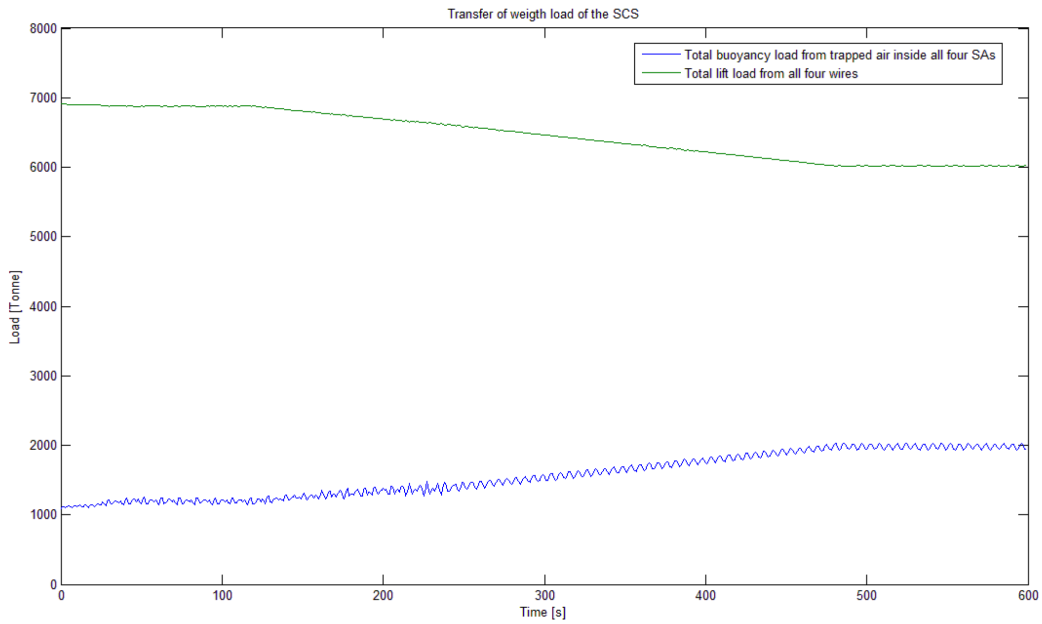


**Figure 44 - Total wire load and total buoyancy load from trapped air**

## 5.2 Discussion of SIMO simulation results

The result of the simulation shows that when the four winches stars to release wire after 120 [s], the weight load stars to transfer from the buoyancy load of the trapped air to the barges until 480 [s] when the winches stop. The wire load in one wire starts at 300 [*tone]*, and after the wire is released the tension has increased to 500 [*tone]*. This is the minimum and maximum wire load specified (chapter 3.1). The heel angle starts at just below 3 [*deg]* and ends just above 5 [*deg]*. A change of heel angle of 2 [deg] is assumed to be acceptable.

The result of Case 1 and Case 2 shows very similar loads and heel angle, expect the wire load. The wire load in one wire or the total wire load of all four wires appears to have some variation, and a close study of the visualization shows the reason. The first order wave forces on the SAs gives the SCS a small oscillating surge motion, and since the wires are relatively short they tend to restrict this motion. This gives the oscillating wire load.

## 5.3 Discussion of the simplified model based on the SIMO simulation

The SIMO model of the lowering operation of the SCS manages to simulate a lowering operation through the sea surface using the simplified model. Both the important depth dependent buoyancy load from the SA's and the heel motion of the barges are successfully modeled. The simulation of the operating shows that the dynamic behavior of the SCS and barges is very small and this implies that the dynamics may be neglected. The simulation of the operation may be viewed as a static problem.

The simplified model is however, not very accurate in worst weather condition. The higher order wave loads such as wave drift load and the wind loads on both the SCS and the barges are not included in the model, and those loads may be large in the worst weather conditions. Only the horizontal first order wave loads on the SAs are included, and not on the rest of the SCS or the barges. The first order wave load should give the SCS an oscillating surge motion, which was consistent with observations of the Case 2 simulation visualization (Chapter A.8). The environmental loads on the SCS and the barges in the simplified model during worst weather conditions are not very accurate.

## 5.4 Discussion of how a model test would improve the SIMO model

A model test of the lowering operation of the SCS was divided into two parts: Part 1 where a model setup of the lowering operation of the SCS through the sea surface were suggested but concluded to not be a good solution. Part 2 where hydrodynamics loads such as added mass and damping where found by performing a decay test.

The result of the SIMO simulations in Case 1 and 2 showed that the operation may be viewed as a static problem. This means that since the problem is not dynamic, the SIMO model does not require added mass and damping. So since the part 1 of the model test cannot be performed, and the results from part 2 is not needed in terms of improving the model, none of the model tests should be required

# 6 Conclusion

## 6.1 Conclusion

The unique method of the lowering operation of the SCS through the sea surface developed by AMC has been defined and the sequence of the lowering operation has been explained. The behavior of the trapped air inside the SAs has been studied and mathematical models to predict this behavior has been derived using the ideal gas law as basis. The speed of the compression and expansion of the trapped air decides if the trapped air follows an adiabatic or isothermal process but for the slow lowering operation this is an isothermal process.

The dimensions of the large and heave SCS and the dimensions of the barges along with other relevant information have been defined. The huge weight of the SCS is the main motivation for the unique method of the lowering operation, as no installation vessel today can install the SCS in one lift.

A simplified model of the complex lowering operation of the SCS through the surface has been developed. This simplified model is the basis for the design basis, and is used to simulate the lowering operation in the time domain program SIMO. Two simulations of the same lowering operation but with and without worst weather waves modeled are performed. The simulations gives the heel angles of the barges, the forces in the wires connecting the barge and the SCS, and the buoyancy forces as the SCS is lowered down.

A model test setup of the lowering operation has been suggested, but modeling the correct behavior of the trapped air in model scale proved very difficult. This model test setup is therefore not recommended and no other alternatives where found. A second model decay test setup to find the hydrodynamic forces on the SCS has also been suggested, and in this test the correct behavior of the trapped air in model scale is successfully included. However, the SIMO simulation of the lowering operation showed that the operation may be viewed as a static problem and not dynamic. The SIMO model does therefore not require added mass or damping as input, and the second model test is therefore not necessary.

## 6.2 Suggestion for further work

The simplified model of the lowering operation of the SCS through the surface do not include the environmental loads very well, and the wind load and the first order wave load along with higher order wave loads should be further studied. No environmental loads on the barges are included, so the two dynamic one mass systems representing the barge heel motions must be developed to include these.

The environmental conditions at the lowering operation site were very roughly estimated. A more thorough investigation would produce much more accurate statistical picture of the likely weather at the site. The wind direction should also be investigated, as this influences the maximum fetch and so the wave height. The result could determine if it is necessary to include environmental loads in the simulation of the operation or not.

Different sequences of the lowering operation procedure should also be investigated. The procedure used in this thesis may not be the optimal one with regards to safety and control of the lowering operation. The results from the simulations in SIMO should also be checked with the same simulations from other time domain programs for validation.

# Bibliography and references

## Literature


[AMC SCS 09] Aker Marine Contractors, ”SCSt Wet Tow Installation by BTA”, Ormen Lange Subsea Compression Conceptual Studies spring 2009

[Faltinsen 09] Odd M. Faltinsen, ”Sea Loads on Ship and Offshore Structures”, Cambridge University press 2009

[Carter 82] D. J. T. CARTER, ”Prediction of wave height period for a constant wind velocity using the JONSWAP results”, Ocean Engineering, 1982, 9, p. 17-33

[Erwing 80] J.A. Ewing, **“**Observations of wind-waves and swell at an exposed coastal location”, Estuarine and Coastal Marine Science Volume 10, Issue 5, May 1980, p. 543-554

[Marin 05] ”TMR 4105 - MARIN TEKNIKK 1”, Trondheim SIT Tapir 2005

[Marin 07] ”TMR 4247 - MARIN TEKNIKK 3”, Trondheim SIT Tapir 2007

[White 05] Frank M. White, ”Fluid Mechanics fifth edition”, Singapore McGraw-Hill 2005.

[Chakrabarti 94] Subrata K. Chakrabarti, “*Offshore Structure Modeling”,.* Singapore World Scientific Publishing Co. Pte. Ltd., 1994.

[Chakrabarti 95] Subrata K. Chakrabarti, “Scale effects on a unique launch sequence of a gravity-based structure”, Chicago, Illinois, USA : s.n., 1995.

[Steen & Aarsnes 08] Sverre Steen and Jan V. Aarsnes, “Experimental Methods in Marine Hydrodynamics”, Trondheim SIT Tapir 2008.

[Moran & Shapiro 06] Michael J. Moran and Howard N. Shapiro, “Fundamentals of Engineering Thermodynamics”, John Wiley & Sons Ltd, 2006.

[DNV 08] DNV-RP-H103 Recommended practice, “Modelling and analysis of Marine operations”, 2008.


## Software documentation


[SIMO theory manual] Harald Ormberg and Halvor Lie, ”SIMO theory manual Version 3.7” MARINTEK, November 4. 2009

[SIMO user manual] Harald Ormberg and Halvor Lie, ”SIMO user manual Version 3.7” MARINTEK, November 4. 2009

[SIMO Appendix A] Harald Ormberg and Halvor Lie, ”SIMO user manual Version 3.7, Appendix A - System Description file” MARINTEK, November 4. 2009

**Conversations and e-mails**

[Johnsgard 10] PhD in Applied Mathematics, Helge Johnsgard
Department manager analyses and engineering, Aker Marine Contractors
PO Box 247, Lilleaker, NO-0216 Oslo, NORWAY
E-mail: helge.johnsgard@akersolutions.com

[Schlömilch 10] Master of Science Stefan Bøyum Schlömilch
Marine Engineer, Aker Marine Contractors
PO Box 247, Lilleaker, NO-0216 Oslo, NORWAY
E-mail: Stefan.Boyum.Schloemilch@akersolutions.com

[Sandvik 10] Head Engineer, Peter Christian Sandvik
Department of Offshore Hydrodynamics, MARINTEK
POB 4125 Valentinlyst, NO-7450 Trondheim, Norway
E-mail: Peter.Sandvik@marintek.sintef.no

[Mo 10] Senior Engineer, Knut Mo
Department of Offshore Hydrodynamics, MARINTEK
POB 4125 Valentinlyst, NO-7450 Trondheim, Norway
E-mail: Knut.Mo@marintek.sintef.no

[Lehn 10] Head Engineer, Erik Lehn
Department of Offshore Hydrodynamics, MARINTEK
POB 4125 Valentinlyst, NO-7450 Trondheim, Norway
E-mail: Erik.Lehn@marintek.sintef.no

[Berg 10] Principal Research Engineer and professor II, Tor Einar Berg
Department of Ship Technology, MARINTEK
POB 4125 Valentinlyst, NO-7450 Trondheim, Norway
E-mail: Tor.Berg@marintek.sintef.no

[Valland 09] Professor, Harald Valland
Marine systems, Department of marine engineering, NTNU
Otto Nielsens vei 10, NO-7052 Trondheim, NORWAY

[Kristoffersen 09] Associate professor, Reidar Kristoffersen
Department of Energy and Process Engineering, NTNU
Kolbjørn Hejes v 1B, NO-7491 Trondheim, NORWAY

**Web pages**

[Eklima] Eklima.met.no
Date: April 14. 2010

[Statkart] http://kart.statkart.no/
Date: Februar 20. 2010

[Google Scholar] http://scholar.google.com/
Date: March 14. 2010

# A Appendices

## A.1 Static barge heel angle calculation

$$\nabla_B = L_B B_B \frac{H_B}{2} \tag{A.1}$$

$$KG_B = \frac{H_B}{2} \tag{A.2}$$

$$KB_B = \frac{H_B}{4} \tag{A.3}$$

$$BM_B = \frac{I_B}{\nabla_B} = \frac{\frac{B_B{}^3 L_B}{12}}{L_B B_B \frac{H_B}{2}} = \frac{B_B{}^2}{6H_B} \tag{A.4}$$

$$GM_B = KB_B + BM_B - KG_B = \frac{2B_B{}^2 - 3H_B{}^2}{12H_B} \tag{A.5}$$

## A.2 HydroD and hand calculation method

The total load on all four SAs for the HydroD and hand calculation model must be calculated. The result from HydroD and hand calculation is for one SA, so the phase lag for the load on the next SA located behind the first one must be accounted for. The two other SAs are also included.

$$kg = \omega^2 \rightarrow \lambda = \frac{gT^2}{2\pi} \tag{A.6}$$

$$\omega = \frac{2\pi}{T_m} = \frac{2\pi\ [rad]}{5.5\ [s]} = 1.142 \left[\frac{rad}{s}\right] \tag{A.7}$$

$X_{SCS} = 30\ m = distance\ from\ center\ of\ one\ SA\ to\ center\ of\ the\ next\ SA$

$\epsilon_1 = phase\ angle\ from\ wave\ to\ load\ on\ first\ SA$

$$\epsilon_2 = \epsilon_1 + \omega \frac{X_{SCS}}{\lambda} T_m = \epsilon_1 + 1.142 \frac{rad}{s} \frac{30[m]}{47.2[m]} 5.5[s] = \epsilon_1 + 3.994\ [rad] \tag{A.8}$$

$= phase\ angle\ from\ wave\ load\ on\ first\ SA\ to\ load\ on\ back\ SA$

$$\zeta_A = \frac{H_S}{2} = \frac{1.84}{2} = 0.92[m] = Wave\ amplitude \tag{A.10}$$

Total load, all four SAs included.

$$F_{waveload} = 2[A_{load}\zeta_A \sin(\omega t + \epsilon_1) + A_{load}\zeta_A \sin(\omega t + \epsilon_2)]$$

$$= 2 \cdot 2A_{load}\zeta_A \sin\left(\omega t + \frac{\epsilon_1 + \epsilon_2}{2}\right) \cos\left(\frac{\epsilon_1 - \epsilon_2}{2}\right) \tag{A.11}$$

$$\sin(\alpha) + \sin(\beta) = 2\sin\left(\frac{\alpha + \beta}{2}\right)\cos\left(\frac{\alpha - \beta}{2}\right) \tag{A.12}$$

$$F_{waveload} = 2 \cdot 2 \cdot A_{load} \cdot 0.92 \sin\left(1.142t + \frac{\epsilon_1 + \epsilon_1 + 3.994}{2}\right)\cos\left(\frac{\epsilon_1 - \epsilon_1 - 3.994}{2}\right) \tag{A.13}$$

$$F_{waveload} = -1.521 \sin(1.142t + \epsilon_1 + 1.997) \tag{A.14}$$

$$F_{waveload,amp} = 1.521A_{load} \tag{A.15}$$

## A.3 MatLab – Key values for different model scale ratios

The MATLAB model test script estimates key values for different model scale ratios. The file is included on the CD in the folder \MatLab script.

## A.4 MatLab – SIMO air spring

The MATLAB SIMO air spring calculates the buoyancy force from equilibrium at a depth of 11 m of a SA. The SA is displaced one meter up and two meters down, and no air is added or released. The file is included on the CD in the folder \MatLab script.

## A.5 Wind data and significant wave height estimation sheet

Wind data measurements from Værnes weather station the last 50 years. The excel sheet used to estimate the significant wav height. The files are included on the CD in the folder \Weather data.

## A.6 All relevant articles

A copy of all the relevant articles found. The files are included on the CD in the folder \Articles.

## A.7 The result of the first order wave force analysis of the SAs

All the results for the first order wave force analysis of the SAs from SIMO – simple model, SIMO – complex model, HydroD and handcalculation. The SIMO – simple model and SIMO – complex model system description files and the command files to run the model in GeniE and HydoD are included. The files are included on the CD in the folder \SA first order wave load results.

| Model name | Depth *[m]* | Result: Load amplitude from software *[MN]* | Result: Corrected load amplitude *[MN]* | File name |
|---|---|---|---|---|
| **SIMO-simple model** | 6 | 6.572 | No corr. req. | SIMO_simple_06.dat |
| **SIMO-complex model** | 6 | 3.777 | No corr. req. | SIMO_complex_06.dat |
| **HydroD** | 6 | 1.509 | 2.295 | HydroD_06.pdf |
| **Handcalc** | 6 | 1.371 | 2.085 | Handcalc_06.dat |
| **SIMO-simple model** | 8 | 7.730 | No corr. req. | SIMO_simple_08.dat |
| **SIMO-complex model** | 8 | 4.509 | No corr. req. | Simo_complex_08.dat |
| **HydroD** | 8 | 1.775 | 2.700 | HydroD_08.pdf |
| **Handcalc** | 8 | 1.602 | 2.437 | Handcalc_08.dat |
| **SIMO-simple model** | 10 | 8.615 | No corr. req. | SIMO_simple_10.dat |
| **SIMO-complex model** | 10 | 5.042 | No corr. req. | SIMO_complex_10.dat |
| **HydroD** | 10 | 1.965 | 2.989 | HydroD_10.pdf |
| **Handcalc** | 10 | 1.771 | 2.694 | handcalc_10.dat |
| **SIMO-simple model** | 12 | 8.500 | No corr. req. | SIMO_simple_12.dat |
| **SIMO-complex model** | 12 | 5.448 | No corr. req. | SIMO_complex_12.dat |
| **HydroD** | 12 | 2.098 | 3.191 | HydroD_12.pdf |
| **Handcalc** | 12 | 1.892 | 2.878 | Handcalc_12.dat |

Table 25- Resulting first order wave force amplitude

## A.8 The SIMO model of the lowering operation of the SCS through the sea surface

The SIMO model of the lowering operation of the SCS through the sea surface, and the results from the simulations with and without waves. The files are included on the CD in the folder \SIMO simulation.